COMPUTATION OF COASTAL MORPHOLOGY

J. WILLILAM KAMPHUIS

Department of Civil Engineering
Queen's University at Kingston
Kingston, Ontario, Canada

1. Introduction

To solve coastal sediment transport and morphology problems, it is necessary to construct a hydrodynamics model to simulate the fluid flow. The hydrodynamics model is then used to calculate sediment transport rates and in turn, these sediment transport rates are used to determine morphology.

The hydrodynamics model is based on the Equation of Motion,

$$\sum F = \frac{d(Mv)}{(dt)} \tag{1}$$

and the Equation of Continuity,

$$\frac{dM}{dt} = 0 \tag{2}$$

where F denotes force, M is mass, v is velocity and t is time.

The forces included in Equation 1 are normally gravity, pressure, bottom friction, lateral exchange of momentum and wave induced forces, although others can be included such as Coriolis force, wind stress, tidal fluctuation, etc. Such a hydrodynamics model normally uses time averaged wave information. The input required for such a model is the complete wave field, everywhere over the calculation domain and estimates of bottom friction and lateral momentum exchange. The output of the model is current velocities and water levels.

The hydrodynamics model can be written to incorporate various levels of sophistication. The most elegant solution uses the Equation of Motion and the Equation of Continuity expressed along three Cartesian co-ordinates, producing a three-dimensional (3-D) model. Properties are defined and computed on a three-dimensional computation grid. To compute sediment transport, it is necessary to use a sediment entrainment function. This is not easy. Most entrainment functions are derived from unidirectional flow over smooth beds. A properly formulated entrainment function must include effects of bottom bedform, accelerations in the flow and liquefaction. To simulate bed morphology, it is necessary to use a conservation of sand mass expression and to repeat the calculation over and over in time. This complete 3-D approach is rarely used in practice because of the large operating costs of such models.

The next lower level of sophistication is a two-dimensional (2-D) model. Two basic types of 2-D models exist. One model assumes that neither velocities nor gradients exist in the alongshore direction. This is normally called a Two-Dimensional (Vertical) model (2-DV). The 2-DV model yields velocities and water levels. Again sediment transport and bed morphology are calculated using an entrainment function and conservation of (sand) mass. Examples of such 2-DV numerical sediment transport models are the cross-shore transport models of Dally and Dean (1984), Stive and Battjes (1984), Stive (1986), Roelvink (1991) and Broker Hedegard et al (1991).

The second type of 2-D model is the Two-Dimensional (Horizontal) model (2-DH). These models use depth integrated versions of Equations 1 and 2. Such a model is normally calculated on a grid with its axes directed parallel and perpendicular to the shoreline. Referring to Figure 1, the 2-DH Equation of Motion may be written (Phillips, 1977) as:

$$\frac{D\vec{u}}{Dt} = -g\vec{\nabla}\eta - \frac{1}{\rho d}\left(\vec{\tau}_b + \vec{\nabla}.S - \vec{\tau}_l\right) \tag{3}$$

where $\vec{\nabla}$ is the horizontal gradient operator, $\vec{u}$ is the horizontal depth-averaged velocity vector, d is the mean water depth (= h + η), h is the still water depth and η is the mean free surface displacement. In this case the forces per unit mass of fluid represented on the right-hand side of Equation 3 are respectively: the hydrostatic pressure force caused by a gradient in mean water level η, shear stress τ_b due to friction on the bottom, the wave-induced force expressed in terms of the gradient of radiation stress tensor S, and the lateral shear stress τ_l also called lateral turbulent mixing.

The continuity equation accounts for the changes in mean water level:

$$\frac{\partial\eta}{\partial t} = -\vec{\nabla}.\vec{q} \tag{4}$$

where $\vec{q} = \vec{u}d$ is the mass flux vector.

In order to solve for the velocity and mean water elevation in a numerical scheme, it is necessary to decompose the velocity vector $\vec{u}$ into its alongshore and on-offshore components, V and U respectively. The axes are defined in Figure 1 and Equations 3 and 4 may be rewritten as:

$$\frac{DU}{Dt} = -g\frac{\partial\eta}{\partial x} - \frac{\tau_{bx}}{\rho d} - \frac{1}{\rho d}\left(\frac{\partial S_{xx}}{\partial x} + \frac{\partial S_{xy}}{\partial y}\right) + \frac{\tau_{ly}}{\rho d} \tag{5a}$$

$$\frac{DV}{Dt} = -g\frac{\partial\eta}{\partial y} - \frac{\tau_{by}}{\rho d} - \frac{1}{\rho d}\left(\frac{\partial S_{xy}}{\partial x} + \frac{\partial S_{yy}}{\partial y}\right) + \frac{\tau_{lx}}{\rho d} \tag{5b}$$

$$\frac{\partial\eta}{\partial t} + \frac{\partial(Ud)}{\partial x} + \frac{\partial(Vd)}{\partial y} = 0 \tag{5c}$$

The left-hand side of Equation 3 represents the total acceleration which may be expressed as the sum of a local and a non-linear convective term:

$$\frac{D\vec{u}}{Dt} = \frac{\partial\vec{u}}{\partial t} + (\vec{u}\ .\ \vec{\nabla})\vec{u} \tag{6}$$

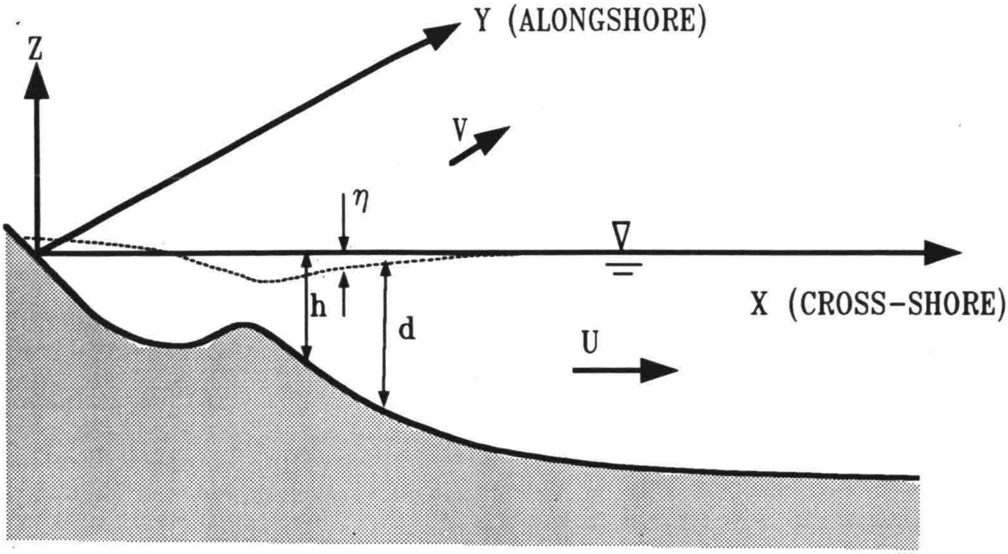

FIGURE 1 CO-ORDINATE AXES FOR QUASI 3-D MODEL

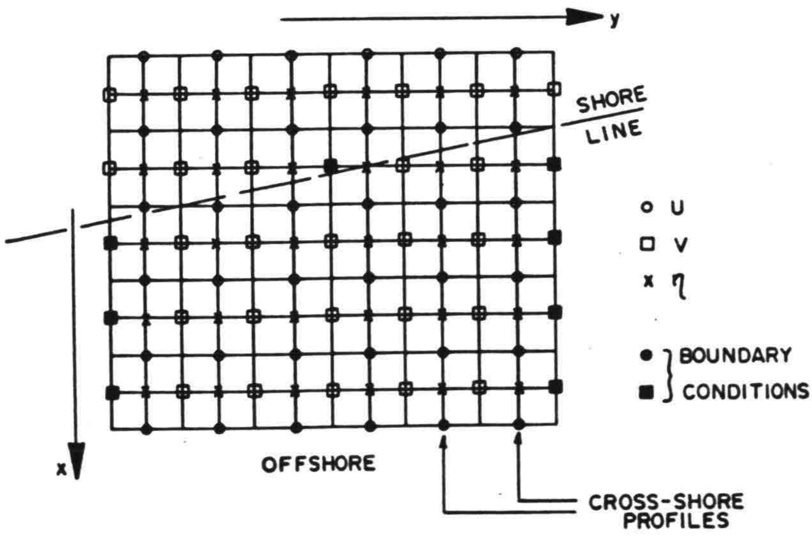

FIGURE 2 COMPUTATIONAL GRID FOR ADI SCHEME

Reviews of such 2-DH models may be found in Basco (1983) and de Vriend (1987). Most models are plagued by stability problems. It is generally agreed that Finite Difference solutions are preferable over Finite Element methods when solving propagational problems. Explicit finite difference solutions do not work well because of the short time steps required, and thus the most efficient method to solve the 2-DH equations appears to be the Alternate Direction Implicit (ADI) scheme. For a staggered grid as shown in Figure 2 values are first calculated for U and η along alternate cross-shore profiles, (i.e. in the X direction) using implicit finite difference approximations of Equations 5a and 5c. This involves iteration from some initial condition. Once U and η have been determined, an implicit finite difference form of Equation 5b, written for the Y direction, calculates V at the alternate profile positions.

The input requirements for the 2-DH hydrodynamic model are similar to the 3-D model. The output is time- and depth averaged velocities in the X and Y directions and time averaged water levels at the grid points. To compute sediment transport in a 2-DH model, the calculated fluid velocities must be combined with wave orbital velocities and introduced into a properly formulated sediment entrainment expression which ideally includes effects of bedform, acceleration and liquefaction. To calculate morphology, a conservation of (sand) mass expression is used and the model is calculated over and over in time.

Because depth averaged velocities are not really related to sediment transport at the bottom, the 2-DH model cannot be very successful as a sediment transport model and the next logical approximation is to re-introduce some vertical structure into the 2-DH model. It is possible to stack 2-DH models for various layers of the flow, but for sediment transport computations a more elegant solution is what is normally identified as a "Quasi Three-Dimensional" model (Q3-D). Examples are Briand and Kamphuis (1990) and Katopodi and Ribberink (1990). Ideally, the vertical structure would itself be calculated using a 2-DV model, but most present Q3-D models still introduce analytically derived expressions for vertical velocity distributions.

2. Example of a Quasi Three-Dimensional Model

As an example, the Q3-D model, by Briand and Kamphuis (1990) will be discussed briefly. This model is discussed in more detail in Briand (1990) and shown schematically in Figure 3.

2.1 GENERAL DESCRIPTION

The underlying hydrodynamic model is based on the 2-DH equations (Equations 5). The calculation domain is divided into a staggered two dimensional horizontal grid as shown in Figure 2. Each of the terms in Equations 5 must be introduced carefully and many versions of the relevant expressions exist.

For bottom friction, some authors introduce non-linear expressions (Ebersole and Dalrymple, 1980, Nishimura, 1981, Watanabe, 1982 and Liu and Dalrymple, 1978). Longuet-Higgins (1970), Liu and Dalrymple (1978), Kraus and Sasaki (1979) and Baum and Basco (1986) introduce linearized formulations. Briand and Kamphuis use the general non-linear expression

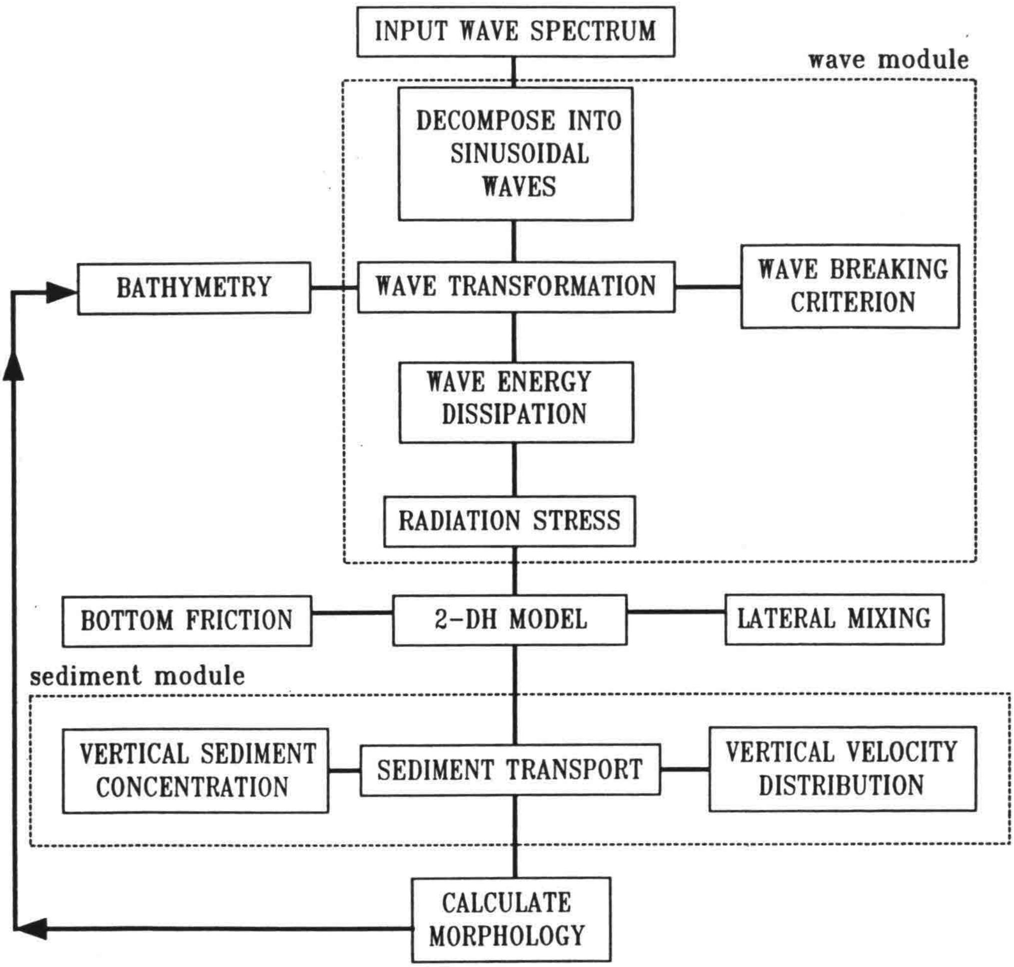

FIGURE 3 QUASI 3-D MODEL LAYOUT

$$\vec{\tau}_b = -\rho\, C_f < |\vec{v}|\vec{v}> \qquad where \quad \vec{v} = \vec{u} + \vec{u}_{wb} \tag{7}$$

The velocity $\vec{v}$ represents the vectorial sum of the depth-averaged current $\vec{u}$ and the instantaneous wave orbital velocity $\vec{u}_{wb}$ at the bottom, ρ is the fluid density, C_f is a time-averaged friction coefficient depending on the bottom roughness and < > means averaged over a wave period.

The wave induced force is normally represented by radiation stress tensor (Longuet-Higgins and Stewart, 1964).

$$S = \begin{bmatrix} S_{xx} & S_{xy} \\ S_{xy} & S_{yy} \end{bmatrix}$$

$$= \begin{bmatrix} \frac{E}{2}\{(3+\cos 2\alpha)\, n - 1\} & E\, n \sin\alpha \cos\alpha \\ E\, n \sin\alpha \cos\alpha & \frac{E}{2}\{(3-\cos 2\alpha)\, n - 1\} \end{bmatrix} \tag{8}$$

where E is the wave energy density, α is the angle of wave approach with the x axis and n is the ratio of wave group velocity over phase velocity. Calculation of these terms is addressed in the next section.

Lateral mixing is introduced using a turbulent eddy viscosity term such as Longuet-Higgins (1970), Jonsson et al (1974), Battjes (1983) or de Vriend and Stive (1987). The model uses de Vriend and Stive's approximation:

$$\nu_t = K_1\, h \left(\frac{D}{\rho}\right)^{1/3} + K_2 \frac{H^2 g\, T}{4\pi^2 h} \cos^2\alpha \tag{9}$$

where D is the energy dissipation rate, H is the wave height and T is the wave period.

Wind induced stresses, Coriolis accelerations and atmospheric pressure gradient terms could be introduced into Equations 5 to complete the calculation, but were not.

Calculations of the Q3-D model of Briand and Kamphuis (1990) proceed as follows:

2.2 WAVE MODULE

The wave driving forces (radiation stress gradients) are computed at each of the grid points.

a. Outside the breaking zone, this involves wave transformation (shoaling, refraction, diffraction, percolation, friction and reflection).

b. In the surf zone, this involves locating and defining the breaker and the energy dissipation rate.

c. Random wave spectra are assumed to be made up of a train of individual sinusoidal waves and the calculations are carried out for each of these.

To model the swash zone, translational velocities resulting from the wave action must be computed.

Because the model needs wave information at regularly spaced grid points and because wave reflection and diffraction are considered to be of secondary importance, the present model calculates wave angles and heights using a domain-based refraction calculation, similar to Perlin and Dean (1983).

Assuming small amplitude waves, refraction is represented by the Wave Propagation Equation:

$$\vec{\nabla} \times \vec{k} = 0 \tag{10}$$

and the Conservation of Wave Energy:

$$\vec{\nabla}(Ec_g) = -D \tag{11}$$

where $\vec{k}$ the wave number vector, c_g the group velocity or speed of wave energy propagation, and D is the energy dissipation rate.

Energy dissipation rate is assumed to be zero outside the breaker zone. For the breaker zone itself, several expressions exist. For regular waves one could use Svendsen (1984), Stive (1984), Sakai et al (1986), or Basco and Yamashita (1986). For random waves Battjes and Stive (1984), Goda (1975) or Leont'ev (1988) could be used. For the present model, the relationship of Dally, Dean and Dalrymple (1984)

$$D = \frac{K_3}{h}\left[\,(E - E_{st})\;c_g\right] \tag{12}$$

was found to yield the best results. Equation 12 is applied to individual wave frequencies in the spectrum, as proposed by Dally and Dean (1986). Recent research at Queen's (Kamphuis, 1993) has found that Equation 12 can be applied directly to wave spectrum using H_s and T_p to define E and c_g. This greatly simplifies calculations. E_{st} is the energy density related to a locally stable wave height as in the work of Horikawa and Kuo (1966).

To delineate the two energy dissipation conditions, it is necessary to define where the breaker occurs and what its characteristics are. The model used Goda (1970) relationship:

$$\frac{H_b}{d_b} = 0.17 \frac{L_o}{d_b} \left\{ 1 - \exp\left[-1.5 \frac{\pi d}{L_o} \left(1 + 15 m^{4/3} \right) \right] \right\} \tag{13}$$

Kamphuis (1991) indicates that for significant breaking wave height, H_{sb}, the coefficient in Equation 13 should be 0.12. He also derives other breaking criteria:

$$H_{sb} = 0.095\ e^{4.0m}\ L_{pb} \tanh(2\pi d_b / L_{pb}) \tag{14}$$

and

$$H_{sb} = 0.56\ e^{3.5m}\ d_b \tag{15}$$

The subscripts s, b, o and p denote "significant", "breaking", "deepwater" and "peak" respectively and m is the beach slope.

2.3 2-DH MODULE

To achieve rapid stability in the ADI calculation, a first estimate for U and η is obtained by assuming an infinitely long beach with parallel bottom contours, i.e., the alongshore gradients of all parameters are zero. (2-DHI calculation). This reduces Equations 5 for any profile (since they are all the same now) to:

$$\frac{\partial U}{\partial t} + U\frac{\partial U}{\partial x} + g\frac{\partial \eta}{\partial x} + \frac{1}{\rho d}\left[\tau_{bx} + \frac{\partial S_{xx}}{\partial x} \right] = 0 \tag{16a}$$

$$\frac{\partial V}{\partial t} + U\frac{\partial V}{\partial x} + \frac{1}{\rho d}\left[\tau_{by} + \frac{\partial S_{xy}}{\partial x} - \frac{\partial}{\partial x}\left(\nu_t \frac{\partial V}{\partial x} \right) \right] = 0 \tag{16b}$$

$$\frac{\partial \eta}{\partial t} + \frac{\partial (Ud)}{\partial x} = 0 \tag{16c}$$

These first estimates of U and η are then introduced into the ADI scheme to solve Equations 5a and 5c. Stable values of U and η and shoreline position at alternate profiles are calculated by iteration (see Figure 2).

When stable values of U and η have been achieved, V is calculated using Equation 5b.

Finally, the calculations using Equations 5a and 5c (to calculate U and η) and Equation 5b (to calculate V) are alternately stepped forward in time until an equilibrium solution is reached for the particular wave condition.

2.4 VERTICAL VELOCITY DISTRIBUTION MODULE

To simulate vertical velocity distribution, the three layer theoretical undertow model by Svendsen and Hansen (1988) was extended. For the surface layer, the volume of fluid contained in the surface roller as expressed empirically by Svendsen (1984a) was used. A thin bottom boundary layer in which fluid viscosity is considered, includes the effect of bottom friction on the flow and accounts for steady streaming due to the wave oscillatory flow. The middle layer flow is governed by the imbalance between the excess momentum flux induced by the breaking wave in the surface layer and the hydrostatic excess pressure created by the local mean water level gradient, or wave set-up.

2.5 SEDIMENT TRANSPORT MODULE

Vertical profiles of wave-induced sediment concentrations in the water column are calculated locally to be combined with vertical profiles of velocities from the vertical velocity distribution module to yield a quasi 3-D sediment transport pattern over the study area.

The vertical profile of sediment concentration is assumed to follow an exponential shape:

$$C(z) = C_A \exp\left(K_4 \frac{(z-z_A)}{z_A} \right) \tag{17}$$

where C is concentration, z is vertical distance above the bottom and the subscript A refers to the top of the bottom boundary layer.

$$K_4 = -\ln(C_B/C_A) \tag{18}$$

where z_A is the bottom boundary layer thickness and C_B is the concentration at which the sediment starts moving as bed load.

The reference concentration C_A at the upper limit of the bottom boundary layer is estimated from a mobility number made up of two terms representing the individual influences of the local wave-current bottom shear stress and the turbulence created by the breaking wave:

$$C_A = \frac{K_5\ (\nu_t/d) + K_6\ (\tau_{wc}/\rho)^{1/2}}{w_f} \tag{19}$$

where K_5 and K_6 are calibration constants, ν_t is the turbulent eddy viscosity, τ_{wc} is the shear stress resulting from waves and currents combined and w_f is the sediment fall velocity.

The above sediment concentration profiles are multiplied by the local velocity profiles and integrated over the depth to yield the local sediment transport rates, in bed-load and suspended load modes.

$$Q_{si} = \int_{z=0}^{h} u_i(z)\ C(z)\,dz \qquad (20)$$

where Q_{si} is the sediment transport rate in direction i. Thus a "Quasi 3-D" description of sediment transport is obtained which is both practical and easy to solve on a micro-computer.

In the swash zone, the sediment transport relationships are not well understood and are still under development for this model. The wave motion in the swash zone is a time-dependent process that is not described by the above numerical model. However, the sediment transport contribution from the swash zone is important as shown in Figure 4 and must be included in some way for comparison with laboratory results. A global formulation based on the assumption that sediment concentration in the swash zone is caused only by wave energy dissipation, is used:

$$Q_{sw} = K_7\,(S_{sw})^{1/6}\ \ (L_{sh})^{1/2}\left(\frac{H_{sh}}{w_f}\right)^{7/3} \qquad (21)$$

where K_7 is a calibration constant, S_{sw} is the swash zone width, L_{sh} is the wave length at the original still water shoreline, H_{sh} is the wave height at the original shoreline.

2.6 MORPHOLOGY MODULE

To calculate bed morphology, the sediment transport rates are introduced into the equation for conservation of (sediment) mass:

$$\frac{\partial Q_{sx}}{\partial x} + \frac{\partial Q_{sy}}{\partial y} = (1-p)\,(\rho_s-\rho)\,\frac{\partial h}{\partial t} \qquad (22)$$

where p is the sediment porosity and ρ_s is the sediment density.

2.7 RESULTS OF CALCULATIONS

The above Q3-D model was calibrated against hydraulic model results and some typical results are shown in Figures 5 to 8.

Figure 5 indicates that the model predicts the wave decay well for both regular and random waves. Figures 6 and 7 show that the alongshore velocities and sediment transport distributions are predicted reasonably well in the surf zone, but in the swash zone the model underpredicts both velocities and

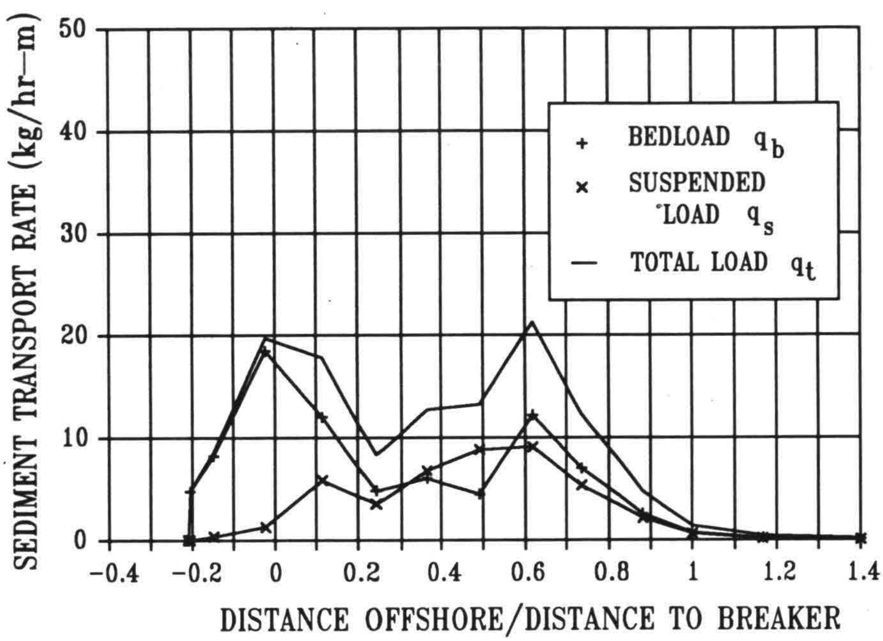

FIGURE 4 TYPICAL ALONGSHORE SEDIMENT TRANSPORT RATE DISTRIBUTION (from Kamphuis, 1991a)

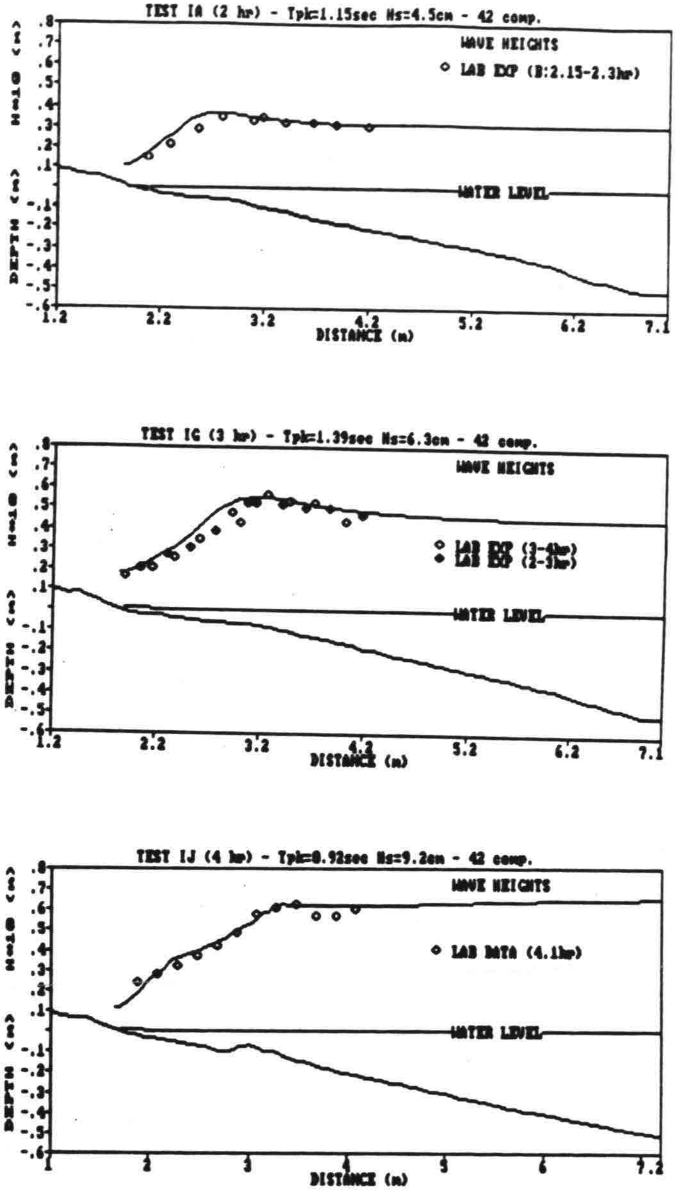

FIGURE 5 PREDICTION OF WAVE DECAY BY QUASI 3-D MODEL
(from Briand, 1990)

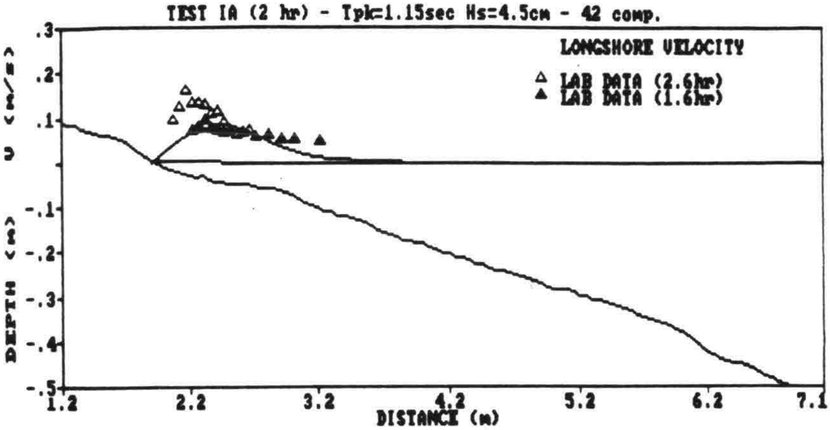

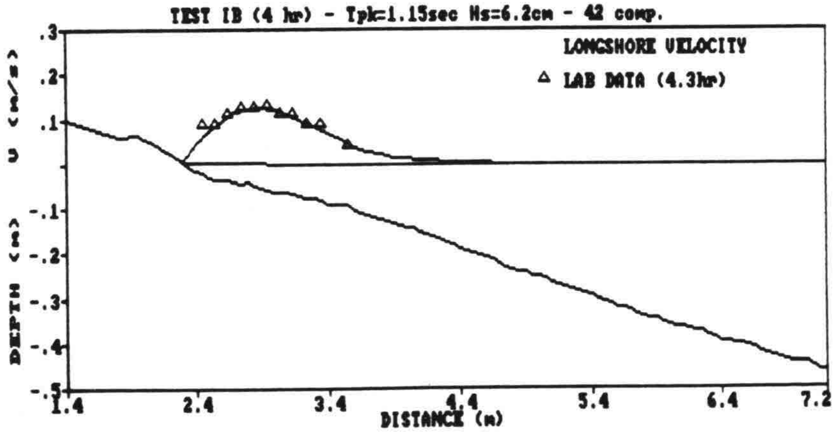

FIGURE 6 PREDICTION OF LONGSHORE CURRENT DISTRIBUTION BY QUASI 3-D MODEL (from Briand, 1990)

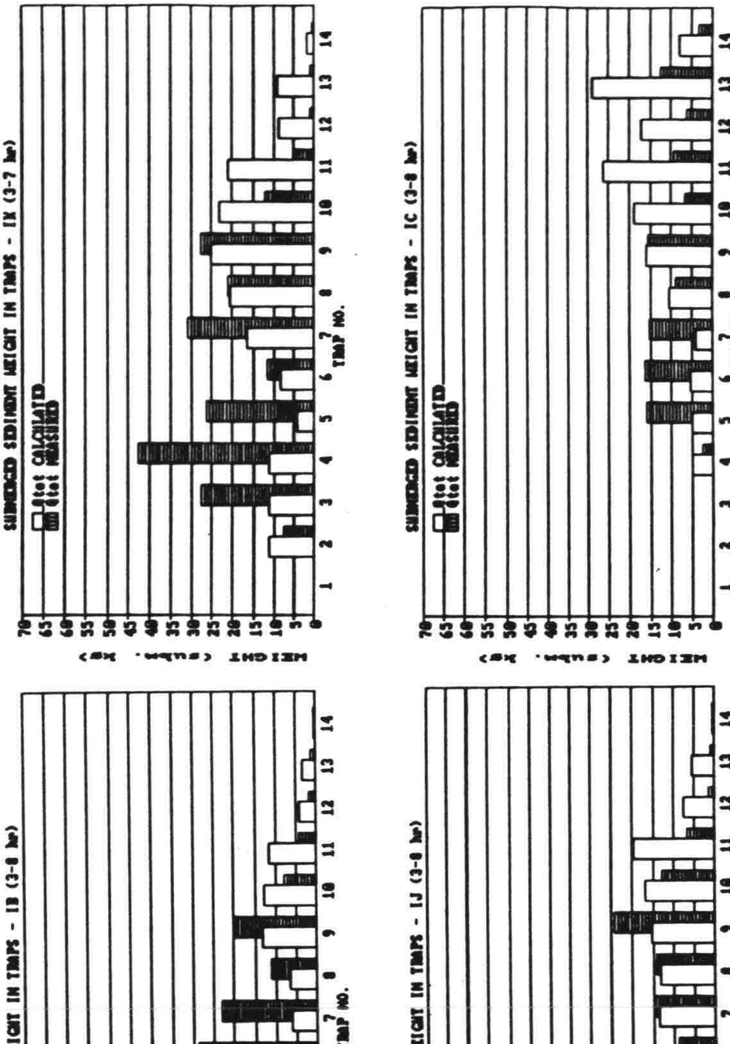

FIGURE 7 PREDICTION OF SEDIMENT TRANSPORT RATE DISTRIBUTION
BY QUASI 3-D MODEL
(from Briand, 1990)

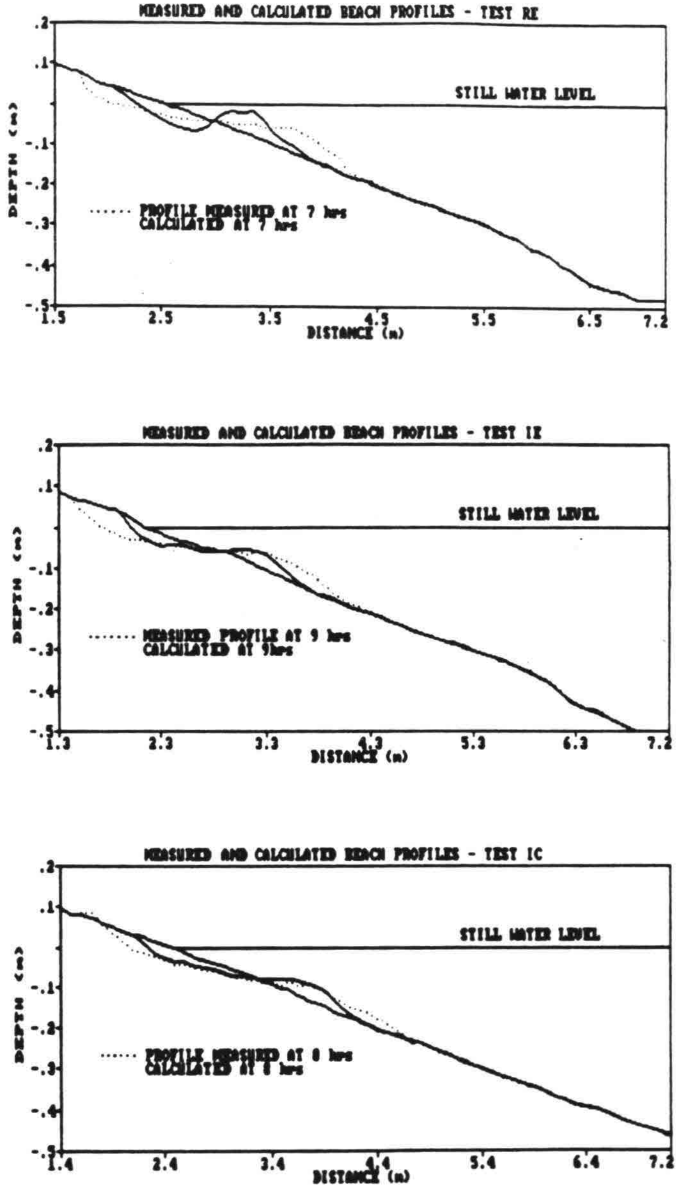

FIGURE 8 PREDICTION OF BEACH PROFILE DEVELOPMENT BY QUASI 3-D MODEL (from Briand, 1990)

sediment transport rates. Obviously more work needs to be done on the important aspect of swash zone transport. Figure 8 demonstrates profile evolution. In general, the swash zone erosion is underpredicted because the swash zone sediment transport rate is too low.

The results certainly look promising and with some more work, the model will be able to perform well and give good results. However, how useful is it for practical engineering computations of shore morphology?

2.8 FRANK DISCUSSION

First of all, the results of a Q3-D model similar to the one discussed here can by definition never come close to reality. Although the Q3-D model incorporates random waves and yield the results typical of field response to irregular incident wave conditions, it has several shortcomings. For example:

a. Calculations are time averaged and do not take into account the effects of variations within a wave period such as wave asymmetry, non-linear wave-wave interactions and sediment transport by infragravity components (e.g. de Vriend, 1991).

b. The influence of bedform on the actual sediment transportation process is not taken into account.

c. Wave diffraction and reflection are not taken into account.

To predict morphology in the vicinity of structures, the domain refraction routine can be replaced by a Refraction-Diffraction calculation. For shore morphology problems, wave reflection is normally small, which means that the computer-hungry Mild Slope Equation for wave transformation (Berkhoff, 1972) can be reduced at least to its Parabolic Approximation (Radder, 1979), perhaps taking into account local reflection with a mirror-imaging scheme. Such a modification would add to the execution time of the model and can only be considered for portions of the model close to structures, leaving the far field wave conditions to be calculated with a refraction calculation.

The Q3-D model, however, is handicapped by much more serious practical limitations than those mentioned above.

First, the model as described above calculates sediment and beach response to one single incident wave condition (although this condition could be represented by a directional wave spectrum). In practice, sediment transport and shore morphology are a response to long term wave conditions. Thus for any practical engineering problem, the calculation would need to be performed many times for wave conditions spanning many years. Such a calculation with a Q3-D model, even for short time series of wave data would quickly become prohibitive for most projects.

At the same time, any long term time series of incident waves is normally based on hindcasts from long term time series of wind. Ideally a wave hindcast has been extensively calibrated against observed wave data, but often that is not the case, yielding very questionable input wave data.

Particularly wave directions are inaccurate (both in the measurements and the hindcast). Yet directional information is absolutely vital in determining coastal circulation and sediment transport and morphology with any accuracy.

With such (normally very poor) input wave data, a repeated, detailed Q3-D calculation of sediment transport is a waste of effort unless one needs to compute detailed sediment transport characteristics such as bar formation or cross-shore velocity or sediment transport gradients, for specific, well known situations.

Finally, the lengthy, involved computations of the Q3-D model may not allow the project engineer to "play" with the model, obtaining a "feel" for the various sensitivities of the computation. Such interactive problem solving techniques are very necessary for coastal morphology problems for which both the basic assumptions and the input data are so poor that sensitivity testing and trial and error methods form a vital part of a proper engineering solution.

Hence, for most practical computations, the sophistication of a repeated 3-D calculation far exceeds the quality of the data while the per-run cost does not allow for the many runs necessary to define vital problem parameters. Hence, a simpler sediment transport and shore morphology calculation which allows many and interactive calculations is very useful.

3. The One-dimensional Model

The remainder of this lecture discusses the simpler one-dimensional model and focusses in detail on the one-dimensional general model "ONELINE" developed specifically to illustrate this lecture. It is a stripped model which performs the basic computations and which must be tailored to each specific problem with its own complexities. Other examples of one-dimensional models are GENESIS (Hanson and Kraus, 1989) and KUST (Willis, 1978).

3.1 THE EQUATIONS

A new set of coordinate axes is introduced (Figure 9).

The One-Dimensional (1-D) model essentially solves two simple simultaneous equations; the equation of conservation of (sand) mass and the equation of (sand) motion.

The first is a 1-D version Equation 22 and will be called the 1-D morphology equation. The second usually takes the form of a "bulk" sediment transport rate expression in which detailed fluid flow relationships are ignored and alongshore sediment transport rate is expressed directly as a simple function of the relevant wave climate and beach characteristics.

3.2 THE 1-D MORPHOLOGY EQUATION

The usual form of the 1-D morphology equation assumes that a beach profile retains constant shape as erosion or accretion takes place, i.e., the profile moves on- or offshore unchanged. The actual beach profile in the calculation can be any shape, as long as the shape moves in the cross-shore direction without change. This means that all the contours move at the same rate and

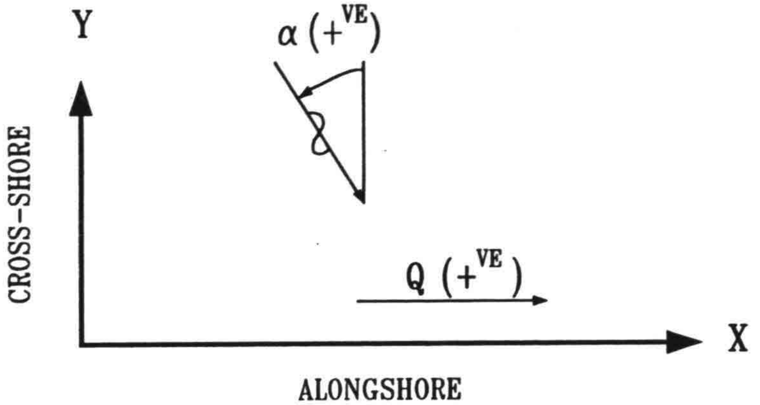

FIGURE 9 CO-ORDINATE AXES FOR 1-D MODEL

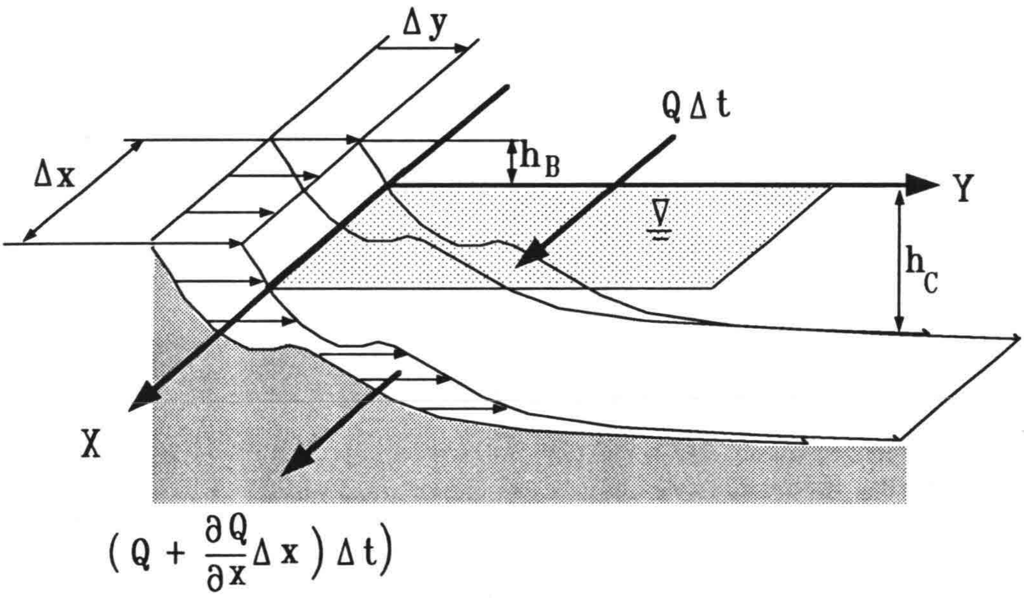

FIGURE 10 BEACH PROFILES AND CONSERVATION OF SAND FOR 1-D MODEL

can be represented by one single contour line as shown in Figure 10. Hence this method is also known as a "1-Line" model. Expressing conservation of (sand) mass as defined in Figure 10 results in:

$$\frac{\partial y}{\partial t} = -\frac{1}{(h_d+h_c)}\left\{\frac{\partial Q}{\partial x} - q_c\right\} \tag{23}$$

where the total depth of the profile, consists of dune (or berm) height (h_d) plus closure depth (h_c), Q is the bulk alongshore sediment transport rate and q_c is the net cross-shore loss of sand per unit distance in the alongshore direction.

The beach profile is essentially assumed to slide along a horizontal base located at closure depth h_c. It is the depth at which beach profiles are not changed by normally occurring wave conditions. This closure depth may be measured from beach profiles. If no measured information is available, closure depth may be estimated from the wave climate using a long-term beach shaping wave height. Following Hallermeier (1981),and making some basic assumptions about beach and wave characteristics, h_c may be estimated as:

$$h_c = 1.6 \quad H_{s,12} \tag{24}$$

where $H_{s,12}$ is the significant wave height that occurs on average 12 hours per year.

3.3 SEDIMENT TRANSPORT RATE

3.3.1 Potential Rate

Alongshore sediment transport rate essentially functions as an integration of all pertinent fluid flow and sediment entrainment properties. Thus its use allows for relatively simple introduction of many years of wave data. Since the input wave data is normally of poor quality, such a simplification is usually justified.

The most commonly used sediment transport rate expression is the CERC expression (Shore Protection Manual, 1984)

$$Q_c = K_c \, H_{sb}^{5/2} \sin 2\alpha_b \tag{25}$$

where Q_c is the CERC rate of sediment transport (m^3/yr), H_{sb} is the breaking significant wave height and α_b is the angle of breaking. The constant K_c is a function of breaking index (H_{sb}/d_b), fluid and sand densities and beach porosity. For a medium dense sand with porosity 0.32 and a breaking index of 0.60 (obtained by using Equation 15), the coefficient is 3.6×10^6.

A more recent expression by Kamphuis (1991a) is more versatile since it takes into account the separate effects of wave height, wave period, wave steepness, wave angle, beach slope and sediment grain size.

$$\frac{Q_i}{\dfrac{\rho H_{sb}^3}{T_p}} = 1.3 x 10^{-3} \left(\frac{H_{sb}}{L_{op}}\right)^{-1.25} m_b^{0.75} \left(\frac{H_{sb}}{D_{50}}\right)^{0.25} \sin^{0.6}(2\alpha_b) \tag{26}$$

where Q_i is the immersed mass of sediment transported (kg/s), T_p is the peak period, m_b is the slope through the breaking zone (d_b/y_b) where y_b is the distance from the shoreline to the breaker and D_{50} is the median grain size of the beach material.

Equation 26 may be expressed more usefully for the present discussion as:

$$Q = K_Q H_{sb}^2 T_p^{1.5} m_b^{0.75} D_{50}^{-0.25} \sin^{0.6}(2\alpha_b) \tag{27}$$

where Q is in m^3/yr and $K = 6.4 \times 10^4$ for a sand with porosity of 0.32.

If a longshore gradient in wave height exists, such as in the shadow of structures, that effect may be incorporated by changing the wave angle term to:

$$[\sin 2\alpha_b - K_8 \frac{1}{m_b} \cos\alpha_b \frac{\partial H_{sb}}{\partial x}] \tag{28}$$

The coefficient K_8 is a matter of discussion (Gourlay, 1978; Ozasa and Brampton, 1980; Kraus and Harikai, 1983). Hanson and Kraus (1989) suggest values of K_8 between 1 and 2.

3.3.2 Actual Rate

Equations 25 and 27 calculate what is known as Potential Sediment Transport Rate, the rate if an infinitely long storm of constant incident conditions acts upon infinite amounts of sand present everywhere. In fact, in most practical cases, storm conditions vary rapidly and the sand is of limited extent and volume. This means the above equations overestimate the Actual Sediment Transport Rate. Normally this discrepancy is taken into account by using K_Q in Equation 27 as a calibration constant to match the calculated rates to actually measured rates. A more elegant method considers the actual limits of sand coverage (Kamphuis, 1990) and will not be discussed here.

3.4 WAVE COMPUTATIONS

3.4.1 Refraction and Breaking

To solve longer-term beach morphology problems,(i.e. many repetitive computations are required) a 1-Line model needs to use relatively simple wave computations. We will discuss a single incoming wave. Adding the effects of many wave conditions to present a practical wave climate is a rather simple matter, once the morphology computations for a single wave condition are understood. Assume this wave approaches with a deep water significant wave height H_{so}, a peak period Tp and an angle of incidence α_0.

Since the bulk sediment transport expressions need input breaking wave conditions, it is necessary to transform the deep water waves:

$$H = K_s K_r K_d H_o \tag{29}$$

where K_s is the shoaling coefficient, K_r the refraction coefficient and K_d the diffraction coefficient. Because each calculation normally must be repeated many times for a single computation and because large simplifying assumptions have been made, the computations must be kept simple and it is normal to use small amplitude wave theory and assume straight, parallel beach contours. This yields:

$$K_s = (C_{go}/C_g)^{1/2} \tag{30}$$

and

$$K_r = (\cos\alpha_o/\cos\alpha)^{1/2} \tag{31}$$

where C_g is the group velocity and α at any location is determined using Snell's Law:

$$\sin\alpha = \frac{C}{C_o}\sin\alpha_o \tag{32}$$

The diffraction coefficient is not important as long as the shoreline is regular (a basic assumption of the 1-Line method anyway) and there are no obstructions to the incoming waves. If offshore structures, long breakwaters or groins are present, it is necessary to include diffraction. In this section we will first treat the case without diffraction.

Equation 29 is valid until the wave breaks. Thus a breaking criterion must be introduced and solved simultaneously with Equation 29. A number of such breaking conditions have been proposed and some are reviewed in Kamphuis (1991). One set of commonly used conditions are a variation of the so-called limiting steepness condition (Miche, 1944)

$$H_b/L_b = 0.14 \tanh k_b d_b \tag{33}$$

where k_b is the breaking wave number ($= 2\pi/L_b$) and L_b is the breaking wave length. Another commonly used set of expressions incorporates the solitary wave criterion Munk (1952).

$$\gamma_b = H_b/d_b = 0.78 \tag{34}$$

Kamphuis (1991) derives two criteria, similar to these expressions and based on from a large series of carefully controlled hydraulic model tests with irregular waves. These have been presented earlier and will be repeated here.

$$H_{sb} = 0.095\, e^{4m}\, L_{pb} \tanh\, (k_{pb} d_b) \tag{14}$$

where L_{pb} and k_{pb} refer to the peak of the spectrum, and

$$H_{sb} = 0.56\ e^{3.5m}\, d_b \tag{15}$$

Note that m is the effective beach slope for the breaking process. This slope is representative of the offshore as well as the breaking zone and is different from m_b in Equation 27.

3.4.2 Diffraction

If offshore structures, long breakwaters or groins obstruct the incoming waves, it is necessary to include diffraction calculations in the 1-Line model. The offshore structures case has been covered in detail in Hanson and Kraus (1989) and other publications related to the "GENESIS" model. As an example, of the type of reasoning and simplifications that go into the development of simplified refraction-diffraction computations, the refraction-diffraction relations near a groin are developed in Appendix I.

Classical calculation of the diffraction coefficient, such as Penney and Price (1951) is lengthy and only applies to regular waves. For example, the Penney and Price method gives a K_d of 0.5 at the edge of the shadow zone, but Goda, Takayama and Suzuki (1978) state this overestimates diffraction for irregular waves. Based on this earlier work, Goda (1985) describes an "angular spreading method" in which it is simply assumed that the obstruction blocks out a portion of the incoming directional wave spectrum. This method arrives at a more reasonable diffraction coefficient of 0.7 at the edge of the shadow zone.

Using Goda's method and some simple additional assumptions, the following simple expressions for refraction-diffraction behind a groin are developed in Appendix I.

Referring to Figure 11, the angle from the shadow line to any point is defined as θ and α_s is the wave angle at the seaward end of the structure.

Using angle θ as parameter, it is possible to approximate K_d as

$$K_d = 0.69 + 0.008\,\theta \qquad \text{for} \qquad 0 \geq \theta > -90 \tag{35}$$

where θ is expressed in degrees, and

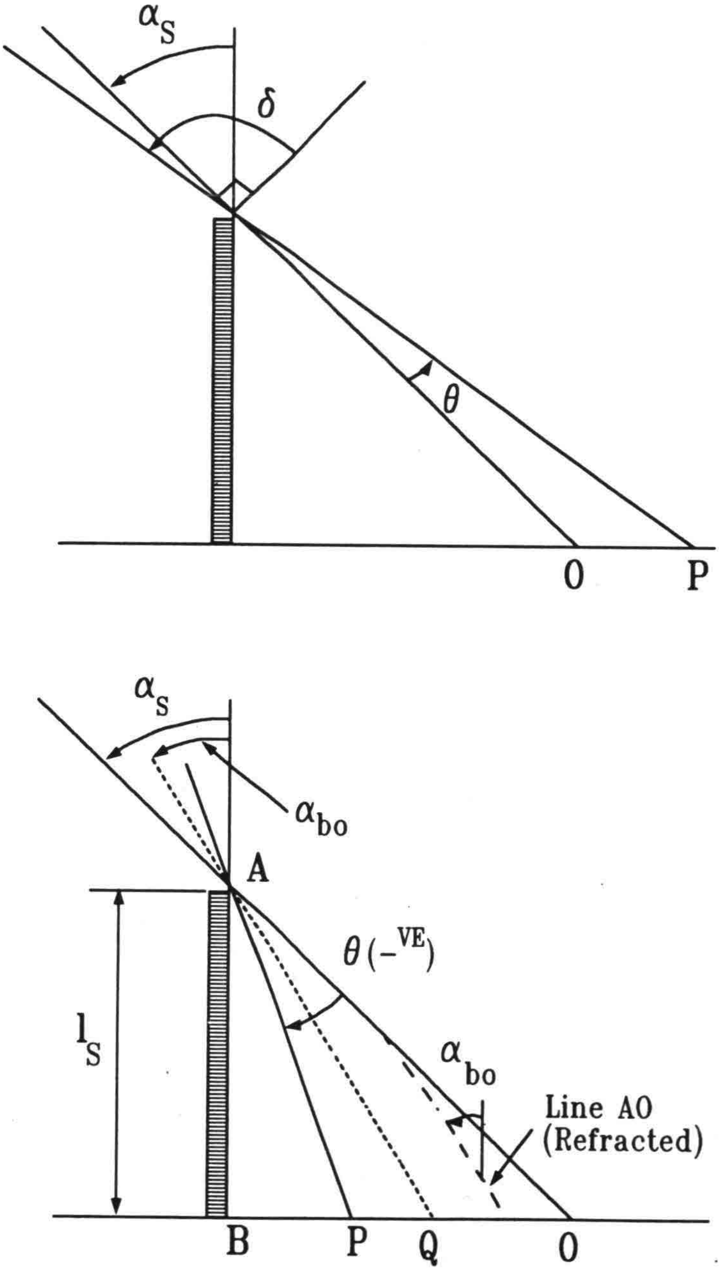

FIGURE 11 REFRACTION-DIFFRACTION APPROXIMATION NEAR GROIN

$$K_d = 0.71 + 0.37 \sin\theta \qquad \text{for} \quad 40 \geq \theta > 0 \tag{36}$$

$$K_d = 0.83 + 0.17 \sin\theta \qquad \text{for} \quad 90 \geq \theta > 40 \tag{37}$$

Breaking wave height may then be estimated by:

$$H_{sb} = K_d \, H_{sbo} \tag{38}$$

where H_{sbo} is the significant breaking wave height without diffraction as determined in the previous section.

The breaking wave angle behind the groin is modified by two processes: diffraction around the structure and additional refraction because the breaking wave height is smaller than without the structure. The combination of these two effects yields:

$$\alpha_{bd} = \alpha_b \, K_d^{0.375} \tag{39}$$

except when

$$\theta < 0 \text{ and } \quad \frac{PB}{I_s} < \frac{1}{2}\{\tan\alpha_s + \tan(0.88\alpha_b)\}$$

in which case

$$\alpha_{bd} = \alpha_b \, K_d^{0.375} \frac{2\,PB}{I_s\{\tan\alpha_s + \tan(0.88\,\alpha_b)\}} \tag{40}$$

Of course, greater sophistication, could be used in the refraction and diffraction computations. However, the poor quality of the input data and the number of assumptions made to arrive at the 1-Line model normally would make greater sophistication unnecessary and the large number of such computations required necessitates this type of "ingenious simplification".

4. Analytical Solutions

To permit an analytical solution of Equations 23 and 25 or 27, boundary conditions must be simple and two basic assumptions must be made.

4.1 EFFECTIVE ANGLE ASSUMPTION

To incorporate the interaction between the waves and changing shoreline configuration, an "effective" breaking wave angle is defined as:

$$(\alpha_b - dy/dx) \tag{41}$$

where α_b is the breaking angle with respect to the basic shoreline "trend" as defined in Figure 9 and dy/dx represents the local shoreline orientation. When this assumption is introduced into Equations 25 or 27 they become:

$$Q = f\ \{\ \sin 2(\alpha_b - dy/dx)\} \tag{42}$$

4.2 SMALL ANGLE ASSUMPTION

This effective wave angle is then further assumed to be small so that

$$Q = f\ \{2(\alpha_b - dy/dx)\} \tag{43}$$

Equation 43 in effect assumes that both α_b and (dy/dx) are small.

Equations 23 and 43 may now be combined into a form of diffusion equation, which has many well known analytical solutions for various imposed boundary conditions.

4.3 EQUATIONS

Pelnard-Considere (1956) solved the diffusion equation for three simple boundary conditions: a complete interruption of the alongshore transport, a bypassing barrier and an instantaneous release of sand on a beach. Le Mehaute and Brebner (1960) also discuss analytical solutions and an excellent recent discussion of those and other analytical solutions may be found in Larson, Hanson and Kraus (1987). They treat several examples of sand supply through beach fills and river discharges and solve shoreline evolution by groins, detached breakwaters and seawalls.

The above 1-Line analytical solutions may be extended to include profiles that change shape. Willis (1977, 1978) proposes a profile that rotates. Bakker (1968) postulates a 2-Line model (Figure 12). This method was derived specifically to calculate the effect of groins on a beach. Essentially, two 1-Line models are stacked together. The connection between the two models is the cross-shore exchange of sediment between them, which according to Bakker is linearly related to the difference between the existing beach profile and its equilibrium shape. Bakker solves these equations for zero net sediment input from external sources in the cross-shore direction.

Other analytical solutions of the 1-Line equations are those by Le Mehaute and Soldate (1978) who included refraction and diffraction and by Borah and Balloffet (1985) who solve the equations for a large incident wave angle.

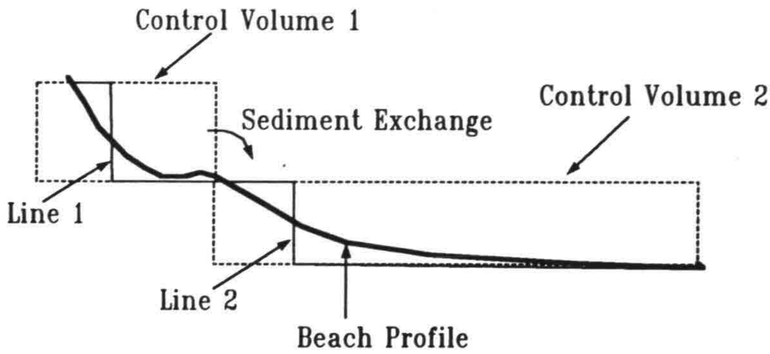

FIGURE 12 TWO LINE MODEL

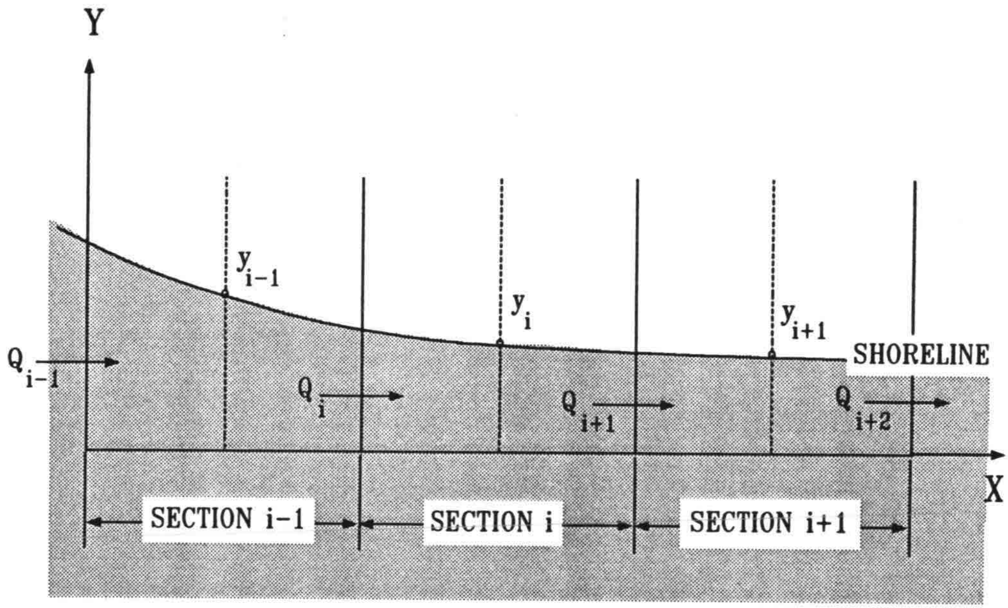

FIGURE 13 DISCRETIZATION OF SHORELINE FOR 1 LINE MODEL

5. Numerical Solutions

5.1 USUAL NUMERICAL SCHEME

If the equations or boundary conditions cannot be simplified sufficiently to result in analytical solutions, Equation 23 together with Equations 25 or 27 must be solved numerically. This can be done for 1-Line and 2-Line models and the scheme may easily be extended to the "N-Line" model (Perlin and Dean, 1983; Johnson and Kamphuis, 1988). The 1-line computation called "ONELINE' which was developed specifically to provide examples for this lecture uses Equations 23 and 27.

Such a 1-Line numerical computation requires the shoreline to be discretized into a series of sections of finite length as shown in Figure 13. Calculation of sediment transport rate, using Equation 27 takes place at the ends of the sections and shoreline position is calculated with Equation 23 at their centres.

The computation uses finite difference techniques and is stepped forward in time using increments of Δt. The finite difference methods are explained in many standard texts, for example Abbott (1979). The simplest finite difference scheme to program is the Explicit Finite Difference Scheme. However, that scheme severely limits the length of the time step that can be used. Once the time step exceeds a limit which may be expressed by a Courant condition, the computation becomes unstable. Implicit Finite Difference Schemes, which are somewhat more difficult to program, do not pose a serious limitation on Δt and are generally used. ONELINE also uses an implicit computation scheme.

For each of the N sections, Equation 23 may be written in finite difference form as:

$$y_i = y_{old,i} - \frac{\Delta t}{(h_d+h_c)\,\Delta x}\,(Q_{i+1} - Q_i - q_c\Delta x) \tag{44}$$

where $y_{old,i}$ is the value of y_i defined or calculated for the previous time increment.

At each of the section ends Q is either specified (as an exterior or interior boundary condition) or calculated using Equation 27. Any implicit method, however, uses (linear) matrix algebra to solve for y and Q simultaneously at each time step. This means Equation 27 must be linear in y and Q. This entails that an implicit solution must make both the effective breaking angle and the small angle assumptions discussed for the analytical solutions, i.e. it uses Equation 43. In Equation 27, Q varies with $[\sin^{0.6} 2\alpha_b]$. To linearize this expression, Equation 43 requires the following further modification and becomes:

$$Q_i = C_i \left\{2\,(\alpha_b - \frac{dy}{dx})_i\right\} \left| 2\,(\alpha_b - \frac{dy}{dx})_i \right|_{old}^{-0.4} \tag{45}$$

where

$$C_i = K_Q \, H_{sb,i}^2 \, T_{p,i}^{1.5} \, m_{b,i}^{0.75} \, D_{50}^{-0.25} \tag{46}$$

and where the subscript (old) refers to previously calculated values. The subscript i is necessary to distinguish between the various sections where the wave conditions will vary because of diffraction.

Equation 45 may be written in finite difference form as:

$$Q_i = \frac{Q_{o,i} - \dfrac{2C_i}{\Delta x}\,(y_i - y_{i-1})}{F_i} \tag{47}$$

where

$$Q_{o,i} = 2 \; C_i \; \alpha_b \tag{48}$$

$$F_i = \left| 2\alpha_b - \frac{2}{\Delta x}\,(y_{old,i} - y_{old,i-1}) \right|^{0.4} \tag{49}$$

Equations 44 and 47, expressed for each of the N shoreline sections results in a tri-diagonal matrix. This matrix is solved easily and rapidly.

$$\begin{bmatrix}
1 & & & & & & & & & & & \\
-A_1 & 1 & A_1 & & & & & & & & & \\
. & -B_2 & 1 & B_2 & & & & & & & & \\
. & . & -A_2 & 1 & A_2 & & & & & & & \\
. & . & . & -B_3 & 1 & B_3 & & & & & & \\
 & & & & & & & & & & & \\
 & & & & & & -B_{N-2} & 1 & B_{N-2} & & & \\
 & & & & & & . & -A_{N-1} & 1 & A_{N-1} & & \\
 & & & & & & . & . & B_{N-1} & 1 & -B_{N-1} & \\
 & & & & & & . & . & . & -A_N & 1 & A_N \\
 & & & & & & . & . & . & . & . & 1
\end{bmatrix}
\begin{bmatrix} Q_1 \\ y_1 \\ Q_2 \\ y_2 \\ Q_3 \\ \\ Q_{N-1} \\ y_{N-1} \\ Q_N \\ y_N \\ Q_{N+1} \end{bmatrix}
=
\begin{bmatrix} R_1 \\ S_1 \\ R_2 \\ S_2 \\ R_3 \\ \\ R_{N-1} \\ S_{N-1} \\ R_N \\ S_N \\ R_{N+1} \end{bmatrix} \tag{50}$$

$$A_i = \frac{\Delta t}{(h_d + h_c)\,\Delta x} \tag{51}$$

$$B_i = \frac{2\,C_i}{\Delta x\,F_i} \tag{52}$$

$$R_i = \frac{Q_{o,i}}{F_i} \tag{53}$$

$$S_i = y_{old,i} + A_i\,q_c\,\Delta x \tag{54}$$

5.2 BOUNDARY CONDITIONS

Two types of boundary conditions may occur - external and internal. The external boundary conditions occur at the two ends of the model and internal ones can occur anywhere within the model.

It is clear from the previous section that for the external boundary conditions, Q needs to be specified. One specification is a constant sediment transport condition at the ends of the model.

$$Q_i = Q \tag{55}$$

This condition indicates that whatever the situation is within the model, the ends for which Equation 55 is specified are not affected; the sediment transport rate there is as if there are no changes in conditions. ONELINE specifies Equation 55 as $Q_{i,\,new}$ and hence incorporates Equation 55 directly into the computational scheme by slightly changing the matrix.

Another boundary condition which may be either external or internal is the complete barrier.

$$Q_i = 0 \tag{56}$$

This condition describes the effect a structure that is sufficiently long to prevent any sediment from passing it.

In time, however, as beach accretes against such a structure, Equation 56 will become invalid and a bypassing condition/needs to be specified. One such expression is developed in Appendix II. It is based on an exponential beach profile shape defined by

$$h = a\,y^{2/3} \tag{57}$$

where a is a profile parameter which is a function of grain size.

The bypassing sediment transport rate is:

$$Q_{by} = Q\left\{1 - \frac{5}{2}\left(\frac{l_e}{y_c}\right) + \frac{3}{2}\left(\frac{l_e}{y_c}\right)^{5/3}\right\} \tag{58}$$

where l_e is the effective structure length

$$l_e = l_s - y_s \tag{59}$$

l_s is the structure length, y_s is the accretion against the structure, and y_c is the distance from the shoreline to the point of intersection of the exponential beach profile with the closure depth h_c.

Equation 58 is only valid until the groin fills up on the one side. At that time the groin condition should be replaced by a constant shoreline position (Equation 64, below). If the groin is filled on both sides, the groin condition must be removed entirely and replaced by a regular shoreline calculation.

Once Equation 57 is used in the computation, it should also be used to define the beach slopes needed in Equations 14, 15 and 27, in order to be consistent. The relevant slopes are derived in Appendix III, resulting in:

$$m = \frac{a^{3/2}}{h_c^{1/2}} \tag{60}$$

$$m_b = \frac{a^{3/2}}{h_{sb}^{1/2}} \tag{61}$$

The above conditions all define Q values.

The shoreline location can also be specified anywhere within the model as a function of time

$$y_i = f(t) \tag{62}$$

6. The Effective Breaking Angle and Small Angle Assumptions

The above description and the usual algorithms for one line modelling are based on the assumptions that both the incident wave breaking angles and the shoreline changes with respect to a general shoreline "trend" are small and that they may be added to give an effective breaking angle. The small angle assumption is, however, not valid in many computations; α_b is large, for example, along the Great Lakes, where the prevailing winds blow along the lake and dy/dx is large for long term computations. Even when all angles are small, it can readily be shown that the effective angle concept leads to incorrect results.

To include non-small α_b or dy/dx in the calculation and to base Q on the actual breaking angle, rather than the effective angle, it is necessary to calculate sediment transport rate explicitly, based on the calculated breaking angle at the particular location and time, i.e. based directly on Equation 27, rather than on Equation 43. Such an explicit calculation causes immediate instability however, for any reasonable time increments.

With ONELINE it was found that stable calculation is possible for reasonable values of Δt through continuing to use the above matrix method. Instead of computing y, however, y_p is calculated, where y_p is the small change in shoreline from the previous shoreline y. This means re-writing Equation 54 as:

$$S_i = A_i q_c \Delta x \tag{63}$$

In this method, y_p and (dy_p/dx) are always small while α_b is defined by the actual shoreline direction (y_{old}) rather than by the "trend" of the shoreline. In addition, the small angle restriction was removed from α_b by reintroducing $\sin \alpha_b$ into Equations 48 and 49. The matrix solution then provides new values of Q and y_p at time $(t+\Delta t)$. The calculated values of Q then are discarded and new values of Q are computed explicitly using Equation 27 with values of y at time $(t+\Delta t)$, where

$$y_{new} = y_{old} + y_p \tag{64}$$

For greater flexibility, it is not necessary in ONELINE to compute Q explicitly, for every Δt. It is possible to specify a ratio of the number of Implicit to Explicit computations to bring about stability or a better fit with measured data. Equation 64 and the explicit computation of Q are used as described above but subsequently a specified number of completely implicit calculations are performed in which y_p (which is still small) is calculated based on the previous value of y_p. The Q calculated by the matrix method is kept as the new Q value for the next computation. Once the specified number of implicit calculations is reached, y is calculated using Equation 64 and Q is calculated explicitly for the next computation. Then the cycle is repeated.

Using alternate implicity and explicit calculations makes good practical sense. In the explicit computation, Q is assumed to be a function of the local value of α_b only as if it does not relate to adjacent Q values. This is physically not correct. The implicit method on the other hand relates Q to adjacent Q values only and no longer to the local α_b. This is also incorrect. The combination of the two yields a stable as well as a sensible solution.

Although this calculation method yields a stable solution for most instances, it still has problems with very large incident wave angles in which a slight change in shoreline direction causes Q to change suddenly from a large value to zero, resulting in almost impossible stability requirements.

ONELINE introduces two simple smoothing procedures to remove such local, quirky shoreline conditions. Such a smoothing procedure is not simply an artifice to bring about a good solution. Smoothing also simulates nature which itself smooths out large local abnormalities. Smoothing does, however, affect the final shoreline position by violating the conservation of (sand) mass. Therefore smoothing should be optimized to result in a smooth, but physically sensible shoreline which is not so smeared out that it no longer represents the practical problem at hand.

The two smoothing options in ONELINE are the application of a simple smoothing function

$$A_i = (A_{i-1} + 2A_i + A_{i+1})/4 \tag{65}$$

where A represents either the computed y values or Q values. Smoothing of y values has more drastic effect on the final solution than smoothing Q values, but in extreme situations both are necessary and the user must be careful to recognize the limitations such smoothed solutions.

7. Examples

Practical examples using ONELINE are presented with this lecture. The shortcomings of programs using the effective breaking angle and small angle assumptions are demonstrated.

The immediate instabilities resulting from a pure explicit solution of Equations 23 and 27 are shown. ONELINE solutions are presented for simple shorelines with simple wave climates and these are compared with analytical solutions. Finally, complicated shoreline examples subjected to multi-year, multi-directional wave climates are treated. The effects of the ratio of Implicit to Explicit computations and the effect of Q and y smoothing are demonstrated.

SYMBOLS

A_i	General parameter
a	Beach profile coefficient
$C(z)$	Vertical time-averaged sediment concentration profile
C_A	Reference concentration at level z_A
C_B	Sediment concentration at initiation of sediment motion
C_f	Time averaged friction coefficient
C_{sw}	Average suspended sediment concentration in the swash zone
c	Wave phase velocity
c_b	Wave phase velocity at breaking
c_g	Wave group velocity
D	Wave energy dissipation rate
D_{50}	Median sediment grain size
d	Mean water depth
d_b	Mean water depth at breaking
E	Wave energy density
E_{st}	Stable wave energy density for a constant depth
F	Driving force term for surf zone currents
g	Gravitational acceleration
H	Wave height
H_b	Breaking wave height
H_o	Deep water wave height
H_s	Significant wave height
H_{sb}	Significant breaking wave height
H_{sh}	Wave height at original shoreline
$H_{s,12}$	Significant wave height occurring 12 hrs/yr
h	Still water depth
h_c	Closure depth
h_d	Dune (or berm) height
K_C	Calibration constant for CERC Bulk sediment transport expression
K_d	Diffraction coefficient
K_i	Constants
K_Q	Calibration constant for Queen's bulk sediment transport expression
K_r	Refraction coefficient
K_s	Shoaling coefficient
k	Wave number
L	Wave length
L_b	Breaking wave length
L_o	Deep water wave length
L_{pb}	Breaking wave length associated with peak period
L_{sh}	Wave length at original shoreline
l_e	Effective structure length
l_s	Structure length
M	Mass of fluid contained in a given control volume
m	Beach slope
m_b	Beach slope in breaking zone (=db/db)
n	Ratio of wave group velocity over phase velocity (= c_g/C)
p	Porosity of sediment
Q	Bulk sediment transport rate (volume)
Q_{si}	Depth- and time-integrated local rate of sediment transport (submerged mass) in the direction of coordinate i
Q_{sw}	Global swash sediment transport rate

q	Mass flux
q_c	Net cross-shore sediment loss per unit distance along shore
S	Wave radiation stress tensor
S_{SW}	Swash zone width
T	Wave period
T_p	Peak period
t	time
U	Horizontal, time-averaged velocity in x-direction
u	Horizontal time- and depth-averaged velocity
u_i	u in direction of coordinate i
u_{wb}	Wave orbital velocity at the bottom
V	Horizontal, time-averaged velocity in y-direction (m/sec)
$\underline{v}$	Velocity
$\vec{v}$	Vectorial sum of current $\vec{u}$ and $\vec{u}_w$
w_f	Sediment fall velocity
x	Horizontal direction (cross-shore in Section 2 and alongshore in Section 3)
Y	Horizontal direction (alongshore in Section 2, cross-shore in Section 3)
y_b	Distance from shoreline to the breaker
y_c	Distance from shoreline to h_c
y_p	Incremental shoreline change
y_s	Accretion against structure
z	vertical axis
z_A	reference level
α	Wave angle of approach
α_b	Breaking wave angle
α_{bd}	Diffracted breaking wave angle
α_s	Wave angle with respect to a structure
γ_b	Breaking index
η	Wave set-up or set-down
θ	Diffraction angle
ν_t	Turbulent eddy viscosity
ρ	Fluid density
ρ_s	Sediment density
τ_b	Shear stress due to bottom friction
τ_l	Lateral shear stress or lateral turbulent mixing
τ_{wc}	Shear stress developed under the combined action of waves and currents

REFERENCES

Abbot, M.B. (1979). Computational Hydraulics: Elements of theory of free surface flows, Pitman Press, 326 pp.

Bakker, W.T. (1968). The dynamics of a coast with a groyne system. *Proc. 11th Int. Conf.Coast. Eng., ASCE*. pp. 492-517.

Basco, D.R. (1983). Surfzone currents. *Coast. Eng.*, Vol. 7, pp. 331-517.

Basco, D.R. and Yamashita, T. (1986). Toward a simple model of the wave breaking transition region in surf zones. *Proc. 20th Int. Conf. Coast. Eng., ASCE*, pp. 955-970.

Battjes, J.A. (1983). Surf zone turbulence. *Symposium on Hydrodynamics of Waves in Coastal Areas, IAHR*, pp. 137-140.

Battjes, J.A. and Stive, M.J.F. (1984). Calibration and verification of a dissipation model for random breaking waves, *Proc. 19th Int. Conf. Coast. Eng., ASCE*, pp. 649-660.

Baum, S.K., and Basco, D.R. (1986). A numerical investigation of the longshore current profile for multiple bar/trough beaches. *Proc. 20th Conf. Coast. Eng., ASCE*, pp 971-985.

Berkhoff, J.C.W. (1972). Computation of combined refraction-diffraction. *Proc. 13th Int. Conf. Coast. Eng., ASCE*, pp. 471-490.

Borah, D.K., and Balloffet, A., (1985). Beach Evolution Caused by Littoral Drift Barrier. *Journal of Waterways, Port, Coastal and Ocean Engrg.*, ASCE, Vol. 111, pp. 645-660.

Briand, M.H.G. (1990). A detailed quasi 3-D numerical model for sediment transport processes in the surf zone. *Ph.D. Thesis Queen's University at Kingston*, 302 pp.

Briand, M.H.G. and Kamphuis, J.W. (1990). A micro computer based quasi 3-D sediment transport model. *Proc. 22nd Int. Conf. Coast. Eng., ASCE*, pp. 2159-2172.

Broker Hedegaard, I., Deigaard, R., and Fredsoe, J., (1991). Onshore/offshore sediment transport and morphological modelling of coastal profiles. *Coastal Sediments '91, ASCE*, pp. 643-657.

Dally, W.R., Dean, R.G., and Dalrymple,R.A. (1984). A model for breaker decay on beaches. *Proc. 19th Int. Conf. Coast. Eng., ASCE*, pp. 82-98.

Dally, W.R. and Dean, R.G. (1986). Transformation of random breaking waves on surf beat. *Proc. 20th Int. Conf. Coast. Eng., ASCE*, pp. 109-123.

de Vriend, H.J. (1987). Two- and three-dimensional mathematical modelling of coastal morphology. *Delft Hydraulics Communications* No. 377.

de Vriend, H.J. (1991). G6 coastal morphology. *Coastal Sediments '91, ASCE*, pp. 356-370.

de Vriend, H.J. and Stive, M.J.F. (1987). Quasi-3D modeling of nearshore currents. *Coast. Eng.*, Vol 11, pp. 565-601.

Ebersole, B.A. and Dalrymple, R.A. (1980). Numerical modeling of nearshore circulation. *Proc. 17th Int. Conf. Coast. Eng., ASCE*, pp. 2710-2725.

Goda, Y. (1970). A synthesis of breaker indices. *Trans. Japan Soc. of Civ. Eng.*, Vol. 2, No. 2, pp. 227-230.

Goda, Y., Takayama, T., and Suzuki, Y. (1978). Diffraction diagrams for directional random waves. *Proc. 16th Int. Conf. Coast. Eng., ASCE*, pp. 628-650.

Goda, Y. (1975). Irregular wave deformation in the surf zone. *Coastal Eng. in Japan*, Vol. 10, pp. 13-26.

Goda, Y. (1985). Random seas and design of maritime structures, *University of Tokyo Press*, 323 pp.

Gourlay, M.R., (1978). Wave-generated currents. *Ph.D. Thesis, Univ.of Queensland, Australia*, 566 pp.

Hallermeier, R.J. (1981). A profile zonation for seasonal sand beaches from wave climate. *Coastal Eng.*, Vol 4, pp. 253-271.

Hanson, H. and Kraus, N.C. (1989). Genesis: Generalized model for simulating shoreline change. *CERC Report 89-19*, US Corps of Engineering, Vicksburg, 185 pp.

Horikawa, K. and Kuo, C.T. (1966). A study on wave transformation inside the surf zone. *Proc. 10th Int. Conf. Coast. Eng., ASCE*, pp. 217-233.

Johnson, H.K. and Kamphuis, J.W., (1988), "N-line model for a large initially conical sand island. *Proceedings Symposium on Mathematical Modelling of Sediment Transport in the Coastal Zone. IAHR*, pp. 275-289.

Jonsson, I.G., Skovgaard, O., and Jacobsen, T.S. (1974). Computation of longshore currents. *Proc. 14th Int. Conf. Coast. Eng., ASCE*, pp. 699-714.

Kamphuis, J.W., (1990). Improving shore protection design. *Canadian Journal of Civil Engineering, CSCE*, Vol 17, pp. 142-147.

Kamphuis, J.W. (1991). Incipient wave breaking. *Coastal Eng.*, Vol 15, pp. 185-203.

Kamphuis, J.W. (1991a). Alongshore sediment transport rate. *Journal of Waterways, Port, Coastal and Ocean Engineering, ASCE*, Vol 117, pp. 624-640.

Katopodi, I, and Ribberink, K. (1990). A Quasi-3D model for suspended sediment transport by currents and waves. *Proc. 22nd Int. Conf. Coast. Eng. ASCE*, pp. 2131-2144

Kraus, N.C., and Harikai, S. (1983). Numerical model of the shoreline change of Oarai Beach. *Coastal Eng.*, Vol 7, pp. 1-28.

Kraus, N.C., and Sasaki, T.O. (1979). Influence of wave angle on the longshore current. *Mar. Sci. Commun.*, 5 (2), pp. 91-126.

Larson, M., Hanson,H., and Kraus, N.C. (1987). Analytical solutions of the one-line model of shoreline change. *CERC Report 87-15*, US Corps of Engineers, Vicksburg, 72 pp.

LeMehaute, B and Brebner, A. (1960). An introduction to coastal morphology and littoral processes. *Queen's University Civil Engineering Report 14*, 44 pp.

LeMehaute, B. and Soldate, M. (1978). Mathematical modelling of shoreline evolution. *Proc. 16th Int. Conf. Coast. Eng. ASCE*, pp. 163-1179.

Leont'ev, I.O. (1988). Randomly breaking waves and surfzone dynamics. *Coastal Eng.*, Vol. 12, pp. 83-103.

Liu, P.L.F., and Dalrymple, R.A. (1978). Bottom frictional stresses and longshore currents due to waves with large angles of incidence, *J. Marine Research*, Vol. 36, pp. 357-375.

Longuet-Higgins, M.S. and Stewart, R.W. (1964). Radiation stresses in water waves; a physical discussion with applications. *Deep-Sea Research*, Vol. 11, pp. 529-562.

Longuet-Higgins, M.S. (1970). Longshore currents generated by obliquely incident sea waves (1 and 2). *J. Geophys. Res.*, Vol. 75, pp. 6778-6801.

Miche, R., (1944). Mouvements ondulatoires des mers en profondeur constante et decroisante. *Ann. Ponts. Chaussees*, pp. 25-78; 131-164; 270-292; 369-406.

Munk, W.H. (1949). The solitary wave theory and its applications to surf problems, *Ann. N.Y. Acad. Sci.* 51 pp.376-423.

Nishimura, H. (1981). Numerical model of nearshore current on a rocky coast. *Nearshore Environment Res. Center Rep.* No. 13, pp. 140-147 (in Japanese).

Ozasa, H., and Brampton, A.H. (1980). Mathematical modeling of beaches backed by seawalls. *Coastal Eng.* Vol 4, pp. 47-64.

Pelnard-Considere, R. (1956). Essai de theorie de l'evolution des formes de rivage en plages de sable et de galets. *4-ieme Journees de l'Hydraulique*, Les energies de la mer, Question III, Rapport No. 1.

Perlin, M. and Dean, R.G. (1978). Prediction of beach platforms with littoral controls. *Proc. 16th Int. Conf. Coast. Eng, ASCE* pp. 1818-1838.

Penney, W.G. and Price, A.T. (1952). The diffraction theory of sea waves and the shelter afforded by breakwaters. *Phil. Trans. Roy Soc. A*, Vol 244(882), pp. 236-253.

Phillips, O.M. (1977). The dynamics of the upper ocean, *Cambridge University Press.*, 261 pp.

Radder, A.C. (1979). On the parabolic equation method for water-wave propagation. *J. Fluid Mech.*, Vol. 95, 1, pp. 159-176.

Sakai, S., Hiyamizu, K., and Saeki, H. (1986). Wave height decay model within a surf zone. *Proc. 20th Int. Conf. Coast. Eng., ASCE* pp. 686-696.

Roelvink, J.A. (1991). Modelling of cross-shore flow and morphology. *Coastal Sediments* '91, *ASCE*, pp. 603-617.

Shore Protection Manual (1984). 4th edition, U.S. Corps of Engineers, Vicksburg.

Stive, M.J.F. (1984). Energy dissipation in waves breaking on gentle slopes. *Delft Hydraulics Lab. Publ.* No. 321.

Stive, M.J.F. (1986). A model for cross-shore sediment transport. *Proc. 20th Int. Conf. Coast. Eng., ASCE*, pp. 1550-1564.

Stive, M.J.F. and Battjes, J.A. (1984). A model for offshore sediment transport. *Proc. 19th Int. Conf. Coast. Eng., ASCE*, pp. 1420-1436.

Svendsen, I.A. (1984). Wave heights and set-up in a surf zone. *Coastal Eng.*, Vol 8, pp. 303-329.

Svendsen, I.A. (1984a). Mass flux and undertow in a surf zone. *Coastal Eng.*, Vol 8, pp. 347-365.

Svendsen, I.A., and Hansen, J.B. (1988). Cross-shore currents in surf zone modelling. *Coast. Eng.*, Vol 12, pp. 23-42.

Watanabe, (1982). Numerical models of nearshore currents and beach deformation. *Coastal Eng. in Japan*, Vol 25, pp. 147-161.

Willis, D.H. (1977). Evaluation of alongshore transport models. *Coastal Sediments '77*, ASCE pp. 350-363.

Willis, D.H. (1978). An alongshore beach evolution model. *Report HY-92*, National Research Council of Canada.

APPENDIX I

COMPUTATION OF DIFFRACTION

In this appendix, some simple equations are developed to calculate refraction-diffraction in the shadow of a breakwater or substantial groin. The structure is assumed to be perpendicular to the shore.

In Figure I-1, the incoming wave ray at the structure makes an angle α_s with the structure. It is desired to calculate the breaking wave conditions at a point which may or may not lie outside the shadow zone defined by the straight line extension of the wave ray from the end of the groin (AO). An angle θ with respect to the shadow line AO is defined as shown in Figure I-1.

Goda (1985) states that analytical methods such as Penney and Price (1951), developed for calculation of diffraction for regular waves, cannot properly describe irregular wave diffraction. Goda proposes instead an "angular spreading method" which simply assumes that part of the directional wave spectrum is blocked by the structure.

He assumes a cosine spreading function and calculates the portion of this energy to which the point of interest is exposed. In Fig. I-1, the portion of energy reaching P is related to angle $\delta = 90 + \theta$. From this, the following table may be drawn up:

TABLE I-1: APPROXIMATE DIFFRACTION COEFFICIENTS

	K_d	
θ	For $\theta \geq 0$	For $\theta \leq 0$
0	0.71	0.71
5	0.75	0.66
10	0.78	0.62
15	0.81	0.58
20	0.84	0.54
25	0.87	0.49
30	0.89	0.45
35	0.92	0.40
40	0.94	0.35
45	0.95	0.32
50	0.96	0.27
55	0.97	0.23
60	0.98	0.20
65	0.985	0.17
70	0.99	0.14
75	0.995	0.10
80	1.0	0.07
85	1.0	0.03
90	1.0	0.00

Regression analysis for the negative values of θ (Figure I-2) yields a very simple relationship:

$$K_d = 0.69 + 0.008\,\theta \qquad \text{for} \qquad 0 \geq \theta > -90 \tag{I-1}$$

where θ is expressed in degrees. Similarly outside the shadow zone (Figure I-3,4) regression analysis yields two strong relationships:

$$K_d = 0.71 + 0.37 \sin\theta \qquad \text{for} \qquad 40 \geq \theta > 0 \tag{I-2}$$

$$K_d = 0.83 + 0.17 \sin\theta \qquad \text{for} \qquad 90 \geq \theta > 40 \tag{I-3}$$

The calculated values of K_d will reduce the wave heights behind the structure and as a result the breaking angle in this area will be reduced, since the breaking wave heights and depths of breaking are smaller.

When this phenomenon was tested for ranges of structure length, α_s, T_p, h_c and γ_b the ratio of the breaking angle adjusted for this diffraction effect (α_{bd}) to the breaking angle without diffraction (α_b) was found not to be sensitive to the variation of all the above parameters. A relationship was then developed between the ratio (α_{bd}/α_b) and K_d as shown in Figure I-5:

$$\alpha_{bd} = \alpha_b \, K_d^{0.375} \tag{I-4}$$

Equation I-4 is valid both inside and outside the shadow zone.

Inside the shadow zone, however, a further decrease in breaking angle resulting directly from wave diffraction must also be taken into account. The wave ray from the end of the groin is refracted and according to Equation I-4 its breaking angle is:

$$\alpha_{bo} = \alpha_b \, (0.71)^{0.375} = 0.88 \, \alpha_b \tag{I-5}$$

It was assumed that this wave ray from the end of the groin, makes landfall halfway between the shadow line AO and the line AQ which makes an angle of α_{bo} with the groin. Since the breaking angle at the structure is zero, a simple proportionality ratio was introduced:

$$\alpha_{bd} = \alpha_b \, K_d^{0.375} \, \frac{2\,PB}{l_s \left\{\tan\alpha_s + \tan(0.88\alpha_b)\right\}} \qquad for \qquad \theta < 0 \tag{I-6}$$

when

$$\frac{PB}{l_s} < \frac{1}{2}\left\{ \tan\alpha_s + \tan(0.88\alpha_b)\right\} \tag{I-7}$$

where l_s is the length of the structure.

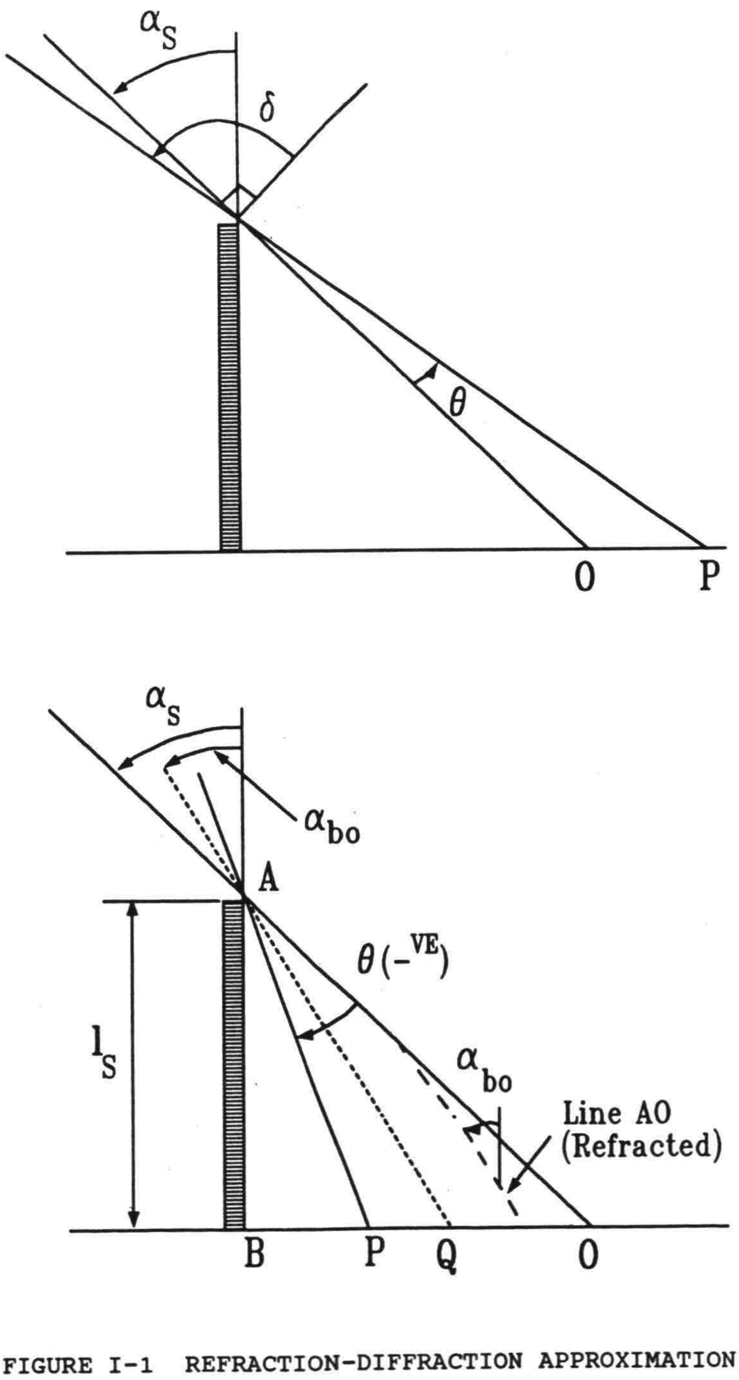

FIGURE I-1 REFRACTION-DIFFRACTION APPROXIMATION NEAR GROIN

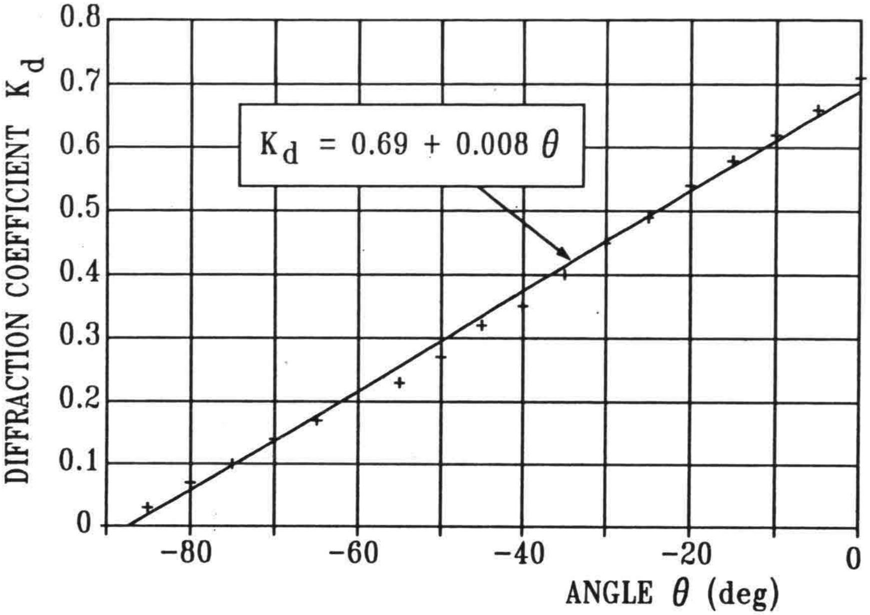

FIGURE I-2 DIFFRACTION COEFFICIENT AS A FUNCTION OF NEGATIVE SHADOW ANGLE

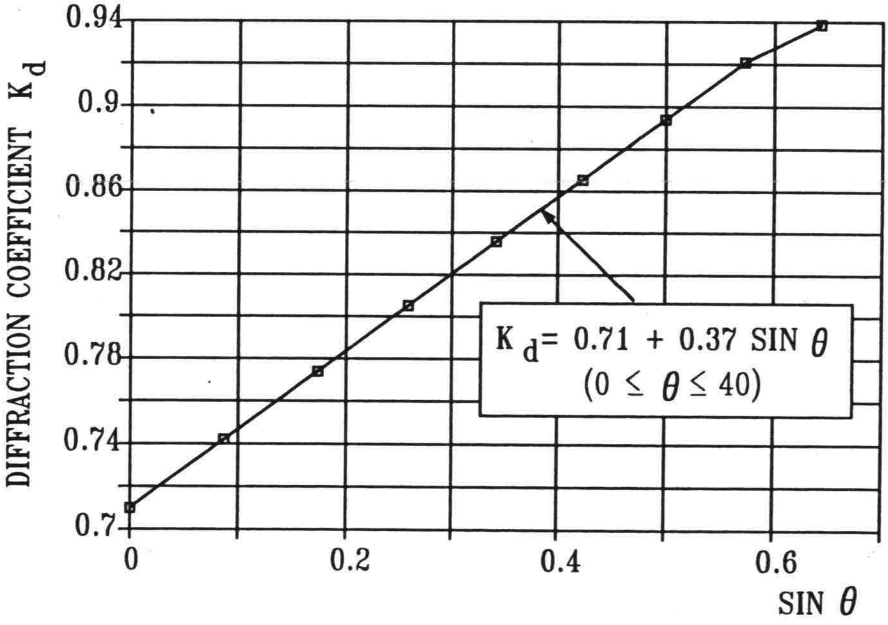

FIGURE I-3 DIFFRACTION COEFFICIENT AS A FUNCTION OF POSITIVE SHADOW ANGLE FROM 0 TO 40 DEGS

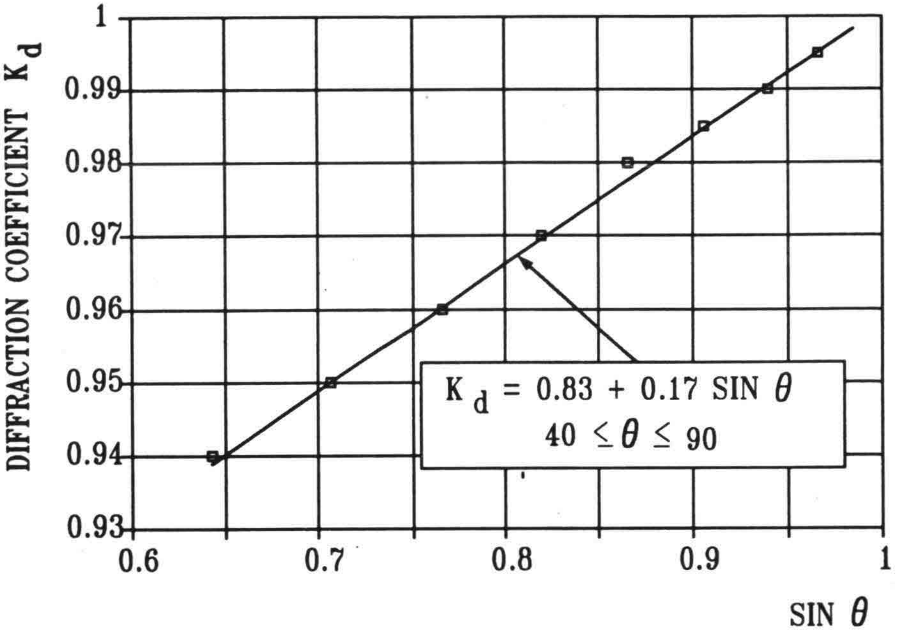

FIGURE I-4 DIFFRACTION COEFFICIENT AS A FUNCTION OF POSITIVE SHADOW ANGLE FROM 40 TO 90 DEGS

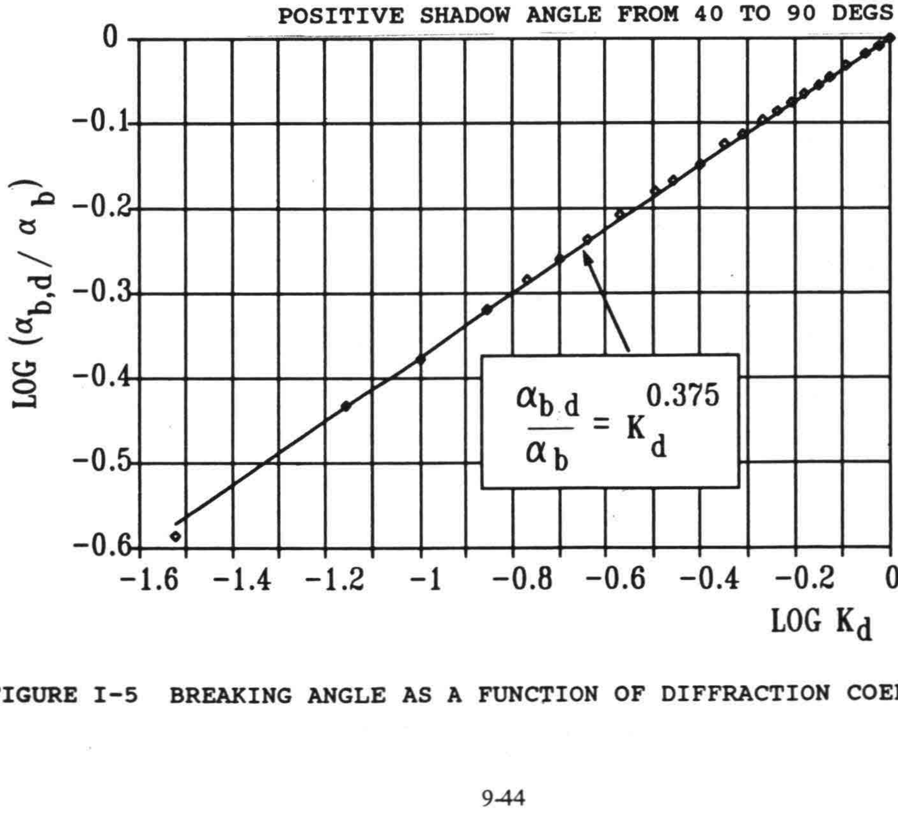

FIGURE I-5 BREAKING ANGLE AS A FUNCTION OF DIFFRACTION COEFFICIENT

APPENDIX II

COMPUTATION OF BYPASSING

If the beach profile shape is assumed to be:

$$h = ay^{2/3} \tag{II-1}$$

and if this shape is assumed to slide along a base at closure depth, h_c then, referring to Figure II-1, the distance to the end of the active profile may be computed as:

$$y_c = \left(\frac{h_c}{a}\right)^{3/2} \tag{II-2}$$

The parameter 'a' is a function of grain size and may be determined from measured profiles. In the absence of measured data, 'a' may be approximated (Hanson and Kraus, 1989) by:

$$\begin{aligned}
a &= 0.41\,(D_{50})^{0.94}, && \text{for} && D_{50} < 0.4 \\
a &= 0.23\,(D_{50})^{0.32}, && \text{for} && 0.4 \le D_{50} < 10.0 \\
a &= 0.23\,(D_{50})^{0.28}, && \text{for} && 10.0 \le D_{50} < 40.0 \\
a &= 0.46\,(D_{50})^{0.11}, && \text{for} && 40.0 \le D_{50}
\end{aligned} \tag{II-3}$$

where a is in $m^{1/3}$ and D_{50} in mm.

The structure has an effective length l_e defined as:

$$l_e = l_s - y_s$$

where l_s is the structure length and y_s is the accumulation of sediment against the structure.
It is assumed that the portion of Q bypassing the structure is related to the ratio:

$$R = \frac{\text{Area of the beach profile above } h_c\text{, between } l_e \text{ and } y_c}{\text{Total area of the beach profile above } h_c}$$

Integration of the profile leads to

$$Q_{by} = Q\left\{1 - \frac{5}{2}\left[\frac{l_e}{y_c}\right] + \frac{3}{2}\left[\frac{l_e}{y_c}\right]^{5/3}\right\} \qquad \text{for } (l_e < y_c)$$

and

$$Q_{by} = 0 \qquad \text{for } (l_e \ge y_c) \tag{II-4}$$

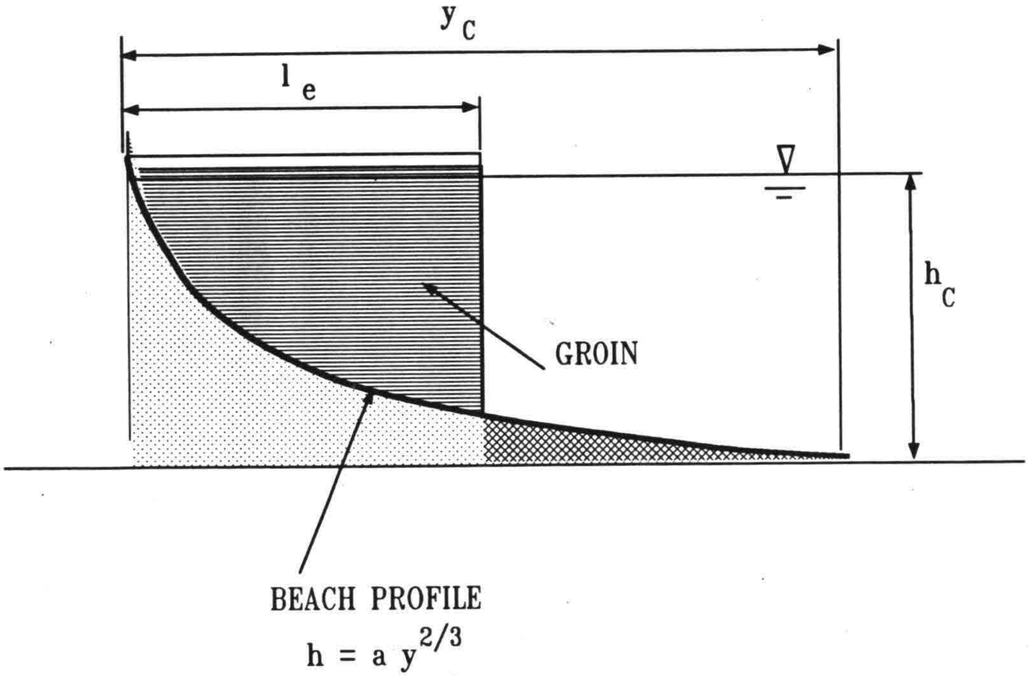

FIGURE II-1 DEFINITIONS FOR BYPASSING COMPUTATION

APPENDIX III

BEACH SLOPE CALCULATION

If the beach profile is assumed to be

$$h = a\, y^{2/3} \tag{III-1}$$

then the relevant beach slopes may be calculated as

$$m = \frac{h_c}{y_c} = \frac{h_c}{h_c^{3/2}}\, a^{3/2} = \frac{a^{3/2}}{h_c^{1/2}} \tag{III-2}$$

and

$$m_b = \frac{h_b}{y_b} = \frac{a^{3/2}}{h_b^{1/2}} \tag{III-3}$$